Received: 24 February 2023 | Revised: 19 May 2023 | Accepted: 1 June 2023

DOI: 10.1002/jmor.21622

RESEARCH ARTICLE

JOURNAL OF morphology WILEY

Differential growth of the adductor muscles, eyeball, and brain in the chick *Gallus gallus* with comments on the fossil record of stem-group birds

Donald G. Cerio[1] | Catherine J. Llera Martín[1] | Aneila V. C. Hogan[1] | Amy M. Balanoff[1,2] | Akinobu Watanabe[3,4,5] | Gabriel S. Bever[1]

[1]Center for Functional Anatomy and Evolution, Johns Hopkins University School of Medicine, Baltimore, Maryland, USA

[2]Department of Psychological and Brain Sciences, Johns Hopkins University, Baltimore, Maryland, USA

[3]Department of Anatomy, New York Institute of Technology College of Osteopathic Medicine, Old Westbury, New York, USA

[4]Division of Paleontology, American Museum of Natural History, New York City, New York, USA

[5]Life Sciences Department, Natural History Museum, London, UK

Correspondence
Donald G. Cerio and Gabriel S. Bever, Center for Functional Anatomy and Evolution, Johns Hopkins University School of Medicine, Baltimore, MD, USA.
Email: donald.cerio@gmail.com and gbever1@jhmi.edu

Funding information
Richard Gilder Graduate School; National Science Foundation; Society of Vertebrate Paleontology; NSF, Grant/Award Numbers: DEB-1947025, DEB-1457181, DEB-1406849

Abstract

The avian head is unique among living reptiles in its combination of relatively large brain and eyes, coupled with relatively small adductor jaw muscles. These derived proportions lend themselves to a trade-off hypothesis, wherein adductor size was reduced over evolutionary time as a means (or as a consequence) of neurosensory expansion. In this study, we examine this evolutionary hypothesis through the lens of development by describing the jaw-adductor anatomy of developing chickens, *Gallus gallus*, and comparing the volumetric expansion of these developing muscles with growth trajectories of the brain and eye. Under the trade-off hypothesis, we predicted that the jaw muscles would grow with negative allometry relative to brain and eyes, and that osteological signatures of a relatively large adductor system, as found in most nonavian dinosaurs, would be differentially expressed in younger chicks. Results did not meet these expectations, at least not generally, with muscle growth exhibiting positive allometry relative to that of brain and eye. We propose three, nonmutually exclusive explanations: (1) these systems do not compete for space, (2) these systems competed for space in the evolutionary past, and growth of the jaw muscles was truncated early in development (paedomorphosis), and (3) trade-offs in developmental investment in these systems are limited temporally to the perinatal period. These explanations are considered in light of the fossil record, and most notably the skull of the stem bird *Ichthyornis*, which exhibits an interesting combination of plesiomorphically large adductor chamber and apomorphically large brain.

KEYWORDS
allometric growth, chicken development, encephalization, jaw adductors, spatial packing constraints

1 | INTRODUCTION

The Constructional School of comparative morphology views organisms as emergent biological machines that reflect the tripartite influence of ecological-adaptive role (i.e., natural selection), historical substrate (i.e., phylogeny), and mechanical or physical constraints (i.e., ahistorical architectural properties; Seilacher, 1970). The vertebrate head, with its myriad neurosensory systems, connective tissues, and feeding-related structures—all residing and functioning within a relatively small area—is fertile ground for employing constructional

principles and testing constructional hypotheses (Biegert, 1957; Gould, 1977; Ross & Ravosa, 1993). One gnathostome lineage where our knowledge of development, morphology, and evolution appears especially poised to reap the benefits of a constructionalist approach is Aves. Compared with other extant reptiles, the bird head is notable for its relatively large brain, with brain-to-body-mass ratios that rival or even surpass those of many mammals (Iwaniuk, 2017; see also Balanoff & Bever, 2017). Birds also have disproportionately large eyes (Walls, 1942), with orbits so large that, in many species, they nearly touch each other through a paper-thin interorbital septum (Martin, 1985). Net expansions of both the brain (sensu stricto) and eyes along the avian stem lineage accompanied a miniaturization in body size that also affected the head (Benson et al., 2014; Lee et al., 2014). As the brain and eyes came to occupy an increasing proportion of an overall diminishing space, one might reasonably predict a diminishing developmental and evolutionary potential for the growth of other functional systems.

Evidence supporting the notion of spatial constraints within the avian head does exist. Encephalization impacts the architecture of the skull roof (Fabbri et al., 2017), and evolutionary shifts in brain orientation and morphology led to anatomical changes in the facial region (Bhullar et al., 2012). Comparative work also established that brain shape differs between birds with differently shaped orbits (Kawabe et al., 2013). Because the brain and eyes scale isometrically with each other in nonpasserine groups (Burton, 2008), this covariation may well reflect competition between these two systems for limited space within the head (Kawabe et al., 2013).

As in cichlid fish, where deeper jaw-adductor musculature is associated with smaller and/or flatter eyeballs (Barel, 1983), it is reasonable to suspect that the adductor musculature of birds was affected, for example, in size or shape, by this trend of increasing relative brain and eye size. However, quantitative tests for trade-offs between cranial neurosensory organs and jaw muscles in birds have not been carried out. It is known that the jaw-adductor chamber in the deep history of birds became apomorphically reduced, relative to the condition in nonavian dinosaurs, as the brain enlarged (Bhullar et al., 2016). Nonetheless, *Ichthyornis*, a Cretaceous stem bird that sits phylogenetically just outside the crown radiation, has both a relatively large (i.e., derived) braincase and a relatively large (i.e., plesiomorphic) adductor chamber (Field et al., 2018). This unexpected combination of traits suggests that the evolutionary and constructional relationships between the adductor chamber and brain are likely to be complicated.

One approach in assessing constructional demands is to track the development of the involved systems (Liem & Wake, 1985; Vogel, 1991). If the avian brain, eyes, and jaw muscles limit each other during their development, we might expect to see relatively large brains associated with relatively small muscles, and vice versa. Although we cannot easily assess developmental dynamics in extinct species except in extraordinary cases of fossilization, we can observe these dynamics in their extant relatives. There has been interest in the homology (e.g., Holliday & Witmer, 2007), size and complexity (e.g., Kalyakin, 2015), and allometry of the jaw-adductor apparatus across bird species (e.g., Navalón et al., 2019), but few ontogenetic series of avian jaw muscles are described outside of Psittaciformes (Tokita, 2004) and a recent study on *Rhea* (Picasso et al., 2023).

Here, we make qualitative and quantitative observations of the jaw-adductor musculature of developing chickens, *Gallus gallus*, and compare these muscles with the size of the brain and diameter of the eye in the same specimens. First, we describe the developmental anatomy of the adductor musculature, paying special attention to any shifts in muscle attachment that occur during ontogeny, which could qualitatively indicate changes in size or shape. Second, we estimate allometric relationships between both absolute and relative measures of size for the brain, eyes, and adductor musculature. Many morphological and physiological traits of muscle, brain, and eyes correlate with body size (Alexander et al., 1981; Bennett, 1996; Bennett & Harvey, 1985; Kiltie, 2000; Maloiy et al., 1979), so the sizes of these organs relative to body dimensions could also yield evidence of trade-offs in space. As body mass data were not available for the sample, we used linear dimensions of the cranium as a metric of overall size. Neurocranium size correlates robustly with body mass in passerines (Shatkovska & Ghazali, 2020), and head width is a reliable proxy for body mass in crocodylians, the sister group to birds (O'Brien et al., 2019), so it is plausible that this trend is a general trait of crown archosaurs. In any event, head size is an appropriate metric to use for this study because multiple organ systems scale with head size (Brooke et al., 1999; Kiltie, 2000).

Finally, we discuss what the observed ontogenetic patterns mean for the influence of spatial packing constraints on the *Gallus* jaw-adductor muscles, visual apparatus, and brain. We also comment on the way our findings relate to the evolutionary history of birds. Ontogenetic series from, for example, anseriform and ratite species would be required to respectively bracket (sensu Witmer, 1995) Galloanserae and Aves, to reveal deeper evolutionary dynamics in the morphology of the avian cranium. However, the data we present here constitute an empirical foundation for future work using a classic model organism, the domestic chicken.

2 | MATERIALS AND METHODS

2.1 | Materials

The sample consists of micro-computed tomography (micro-CT) data of 18 specimens of White Leghorn chicken *Gallus gallus domesticus* Linnaeus, 1758. The specimens represent nine ontogenetic stages ranging from embryonic day 5 to somatically mature adult. All specimens were supplied by Charles River Laboratories. Embryonic specimens were aged embryonic days 9, 12, 15, and 18. Postnatal specimens were 1 day, 1 week, 3 weeks, 6 weeks, and at least 35 weeks of age. Each developmental stage is represented by two individuals (i.e., $N = 2$ per age). Additional micro-CT data of two specimens at embryonic day 5 and two specimens at embryonic day 6 were also studied but measurements of their soft tissues were not tractable due to the absence of staining of

musculature and deformation of the neurosensory organs from stain-related shrinkage. All specimens at embryonic day 18 and older were male; sexes of early embryonic stages could not be assessed. Specimens were euthanized by Charles River Laboratories via cervical dislocation and decapitation, followed immediately by submersion into 10% neutral-buffered formalin solution (see also Hogan et al., 2020; Watanabe et al., 2019, 2021). The Institutional Animal Care and Use Committee at the American Museum of Natural History on March 24, 2014 approved the use of these specimens. See Watanabe et al. (2019) for more details on the sampling of hatchling and older specimens.

Several steps were taken to stabilize specimens before conventional CT imaging, and a staining agent was used to enhance contrast in subsequent imaging. Embryonic specimens were previously stabilized (Hogan et al., 2020) using a hydrogel solution and stained with Lugol's iodine solution (iodine potassium iodide) following established protocol (Carlisle et al., 2017; Carlisle & Weisbecker, 2016; Gignac et al., 2016; Wong et al., 2013). Postnatal specimens were previously fixed in formalin for over 8 weeks before imaging to mitigate the distortion of soft tissues and also stained with iodine potassium iodide (Watanabe et al., 2019). Conventional CT scans were acquired before staining with iodine potassium iodide. Diffusible iodine-based contrast-enhanced computed tomography (diceCT) scans were then obtained to visualize the soft-tissue morphology (Gignac et al., 2016). For additional details on the staining protocol and CT-scan parameters, see Table 1 in Hogan et al. (2020) and Table 1 in Watanabe et al. (2019).

2.2 | CT analysis

Jaw-adductor muscles (Table 1), brains, and cranial bones of each specimen were digitally dissected (segmented) in Amira 6.3.0 (Thermo Fisher Scientific; Figure 1). Skulls were not segmented en

TABLE 1 Names of jaw-adductor muscle groups and individual muscles within those groups.

Muscle group	Muscles within groups
Musculus adductor mandibulae posterior (mAMP)	Two bellies, one lateral and one medial
Musculus adductor mandibulae externus (mAME)	Musculus adductor mandibulae externus superficialis (mAMES)
	Musculus adductor mandibulae externus medialis (mAMEM)
	Musculus adductor mandibulae externus profundus (mAMEP)
Musculus adductor mandibulae internus (mAMI)	Musculus pseudotemporalis superficialis (mPSTs)
	Musculus pseudotemporalis profundus (mPSTp)
	Musculus pterygoideus dorsalis and ventralis (mPTd and mPTv)

Note: Abbreviations are in parentheses.

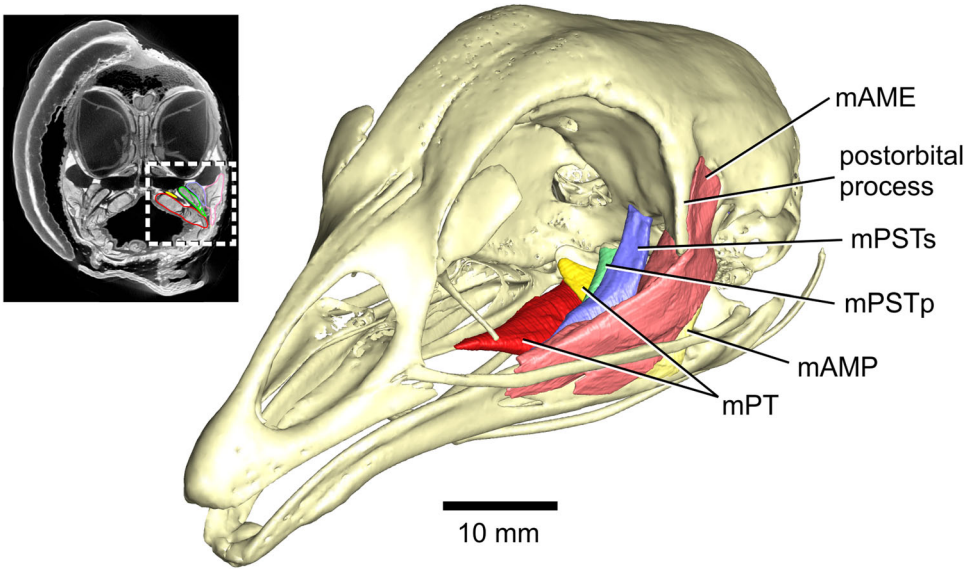

FIGURE 1 Three-dimensional surface models of the jaw-adductor musculature of an adult chicken, *Gallus gallus*, in place with the skull. Inset: a slice from the diceCT scan of this specimen, with segmented muscles highlighted by the white box. diceCT, iodine-based contrast-enhanced computed tomography; mAME; musculus adductor mandibulae externus; mAMP, musculus adductor mandibulae posterior; mPSTp, musculus pseudotemporalis profundus; mPSTs, musculus pseudotemporalis superficialis; mPT, musculus pterygoideus.

masse from prenatal specimens due to dearth of ossification, but skulls and scleral ossicle rings in hatchling and older specimens were extracted using the "Magic wand" tool. Muscles were identified following homologies established in Holliday and Witmer (2007). Each muscle belly (if clearly identifiable) or muscle group was extracted by manually segmenting every 5–10 slices, interpolating, and finally manually editing the resulting volume to correct artifacts introduced by interpolation. Brains were segmented, in a similar manner as the muscles, by gross regions: left and right cerebra, left and right olfactory bulbs, cerebellum, midbrain, and hindbrain. These divisions of the telencephalon and whole brain follow Boire and Baron (1994). Segmentation of the hindbrain was terminated at the deep margin of the foramen magnum. The olfactory bulbs were delineated by the border of the inner periventricular edge and the outer border of the olfactory fila, and the segmented olfactory bulbs do not include CN1.

Anatomical traits of muscles that were noted in the present study included patterns of differentiation (i.e., from muscle primordia), spatial dispositions of proximal and distal attachments to bones, and general morphology. Three-dimensional surface models of muscles, muscle primordia, and skull bones were digitally rendered in Amira. Surface models of soft tissues were used in conjunction with segmented bones to describe the anatomy of the jaw-adductor chamber across the developmental stages.

Additionally, sizes of the adductor muscle group, brain, and eyes were measured (Supporting Information 1). The following quantities were recorded: (1) volume of the brain, obtained by adding together the volumes of all segmented brain regions, (2) volume of each individual muscle, (3) volumes of larger muscle groups musculus adductor mandibulae posterior (mAMP), musculus adductor mandibulae internus (mAMI), and musculus adductor mandibulae externus (mAME), (4) total adductor volume, obtained by adding together the volumes of mAMP, mAMI, and mAME, and (5) equatorial diameter (i.e., rostrocaudal length) of the eye. Volumes were measured in Amira with the Material Statistics module. The 3D Measure tool from Amira was used for linear measurements of the skull and eyeballs in the prestained CT data sets. Linear dimensions of the skull included interquadrate distance (i.e., width of the skull, measured between the lateralmost points of the left and right quadratojugal junctions) and length of the braincase.

2.3 | Ontogenetic scaling of jaw adductors, brain, and eyeballs

The first question we aimed to address in this section of the study was in what way (if any) did the raw growth of the jaw-adductor musculature differ from that of the brain and eyes throughout ontogeny. Our primary alternate hypothesis (H1) was that the growth trajectories of these three systems would differ from one another, with a null of no difference. Growth curves for adductor muscle growth (total adductor musculature volume vs. time), brain growth (brain volume vs. time), and eye growth (diameter vs. time) were created to visualize the development of the three systems and identify any differences in their growth trajectories.

Our second question was in what way (if any) could the size of the jaw-adductor musculature—both in total and separated into component parts—be accounted for by brain or eye size. We conducted several regression analyses to examine the relationship between these two variables. First, we conducted a bivariate regression in R (v.4.1.3) between total adductor volume and either brain volume or eye diameter (R Core Team, 2022). Both ordinary least-squares (OLS) and reduced major axis (RMA) regression parameters were output for comparison. The R packages {lmodel2} (Legendre, 2018) and {smatr} (Warton et al., 2012) were used to estimate the regression parameters and 95% confidence intervals. Second, we used OLS regression analysis in R to estimate the following allometric relationships: (1) head width versus adductor volumes, (2) head width versus brain volume, (3) braincase length versus adductor volumes, (4) braincase length versus brain volume, (5) head width versus eye diameter, and (6) braincase length versus eye diameter. The cube roots of volumes were taken and all variables were also log-transformed before regression analyses. We applied both transformations so that the null hypothesis of slope in the bivariate regressions would be equal to 1 (i.e., isometry of linear dimensions) and the alternate hypothesis (H2) would be a slope different than 1 (i.e., positive or negative allometry). We explicitly tested for differences from isometry using the "linearHypothesis" command in the {car} package (Fox & Weisberg, 2019) in R. After running the regressions, we extracted the residuals (i.e., relative adductor and brain volumes) from each of these relationships. Finally, we ran a new set of partial regression analyses in R, using relative brain volume or relative eye size as the predictor variable and relative adductor volumes as the response variables. The presence of an inverse relationship between these relative dimensions would be evidence in support of spatial trade-offs.

Our third research question was whether the three groups of jaw-adductor muscles (mAME, mAMI, and mAMP) differed in their rate of growth relative to the brain during development. The null hypothesis was no difference, and the alternate hypothesis was a difference in slope among the groups (H3). We performed Analysis of Covariance on allometric regressions derived from the second research question to test for differences in this rate among the groups.

Our fourth and final research question was whether and how the size of the eyeball could be accounted for by the size of the brain. We conducted a final set of bivariate regressions between brain volume and eye diameter. Both OLS and RMA regression parameters were estimated. The null was isometry, and the alternate was a slope different from isometry (H4). Finally, we ran a set of partial regression analyses in R, using relative brain volume as the predictor variable and relative eye diameter as the response variable. The presence of an inverse relationship between these relative dimensions would be evidence in support of spatial trade-offs.

The R scripts for all of our analyses are available in Supporting Information 2.

3 | RESULTS

3.1 | Description of chick adductor musculature development

We identified the following muscles and muscle groups of the jaw-adductor complex in developing chick embryos as young as embryonic day 9: mAME, mAMP, musculus pseudotemporalis superficialis (mPSTs), musculus pseudotemporalis profundus (mPSTp), and musculus pterygoideus (mPT; Figure 1). We describe each muscle group separately in the following sections. Surface mesh reconstructions of the muscles are available in Supporting Information 3–9.

3.1.1 | Musculus adductor mandibulae posterior

This muscle extends from the rostral face of the quadrate bone to the dentary. It is composed of a medial and lateral belly in Galloanserae (Holliday & Witmer, 2007), but these two bellies are challenging to distinguish in the CT data of specimens younger than the third-week post-hatching. In the two specimens at embryonic day 9, the mAMP primordium is distinguishable as a flat, triangular wedge of tissue, about 1 mm in length, located just medial to the caudoventral surface of the eyeball. This muscle sits lateral to the mPT primordium, medial to the mAME primordium, and caudal to the mPST primordia (Figure 2). We did not observe muscle fibers in the CT-scan data at this age.

Regional differences become clearer between the medial and lateral halves of mAMP by embryonic day 18, though these halves are not separable in the CT data. The medial half of mAMP is robust and short, about 2 mm long. This part of the muscle stretches from the ventrolateral aspect of the orbital process of the quadrate to the dorsal surface of the dentary. The attachment on the dentary extends across the dorsomedial and dorsolateral faces of the bone, just caudal to the attachments of mPSTs and mPSTp to the dentary. The lateral half of mAMP is thinner but longer, about 5 mm in length. This part of the muscle stretches from the body and otic process of the quadrate to the lateral surface of the dentary. At its lateral attachment, this part of mAMP is caudal to the attachment of mAME.

In older specimens, the overall form of mAMP does not differ from the muscle in specimens at 18 days, except that the medial and lateral bellies in older specimens are more clearly distinguishable in CT slice data. However, we noted that mAMP has a more lateral component to its orientation in older specimens than in younger specimens (Figure 3). This change in orientation is accompanied by the mandible growing more robust and mediolaterally broader relative to the braincase.

3.1.2 | Musculus adductor mandibulae internus

This muscle group is mostly contained within the palatal region of the chick skull (Figure 4), and it is composed of multiple muscle bellies.

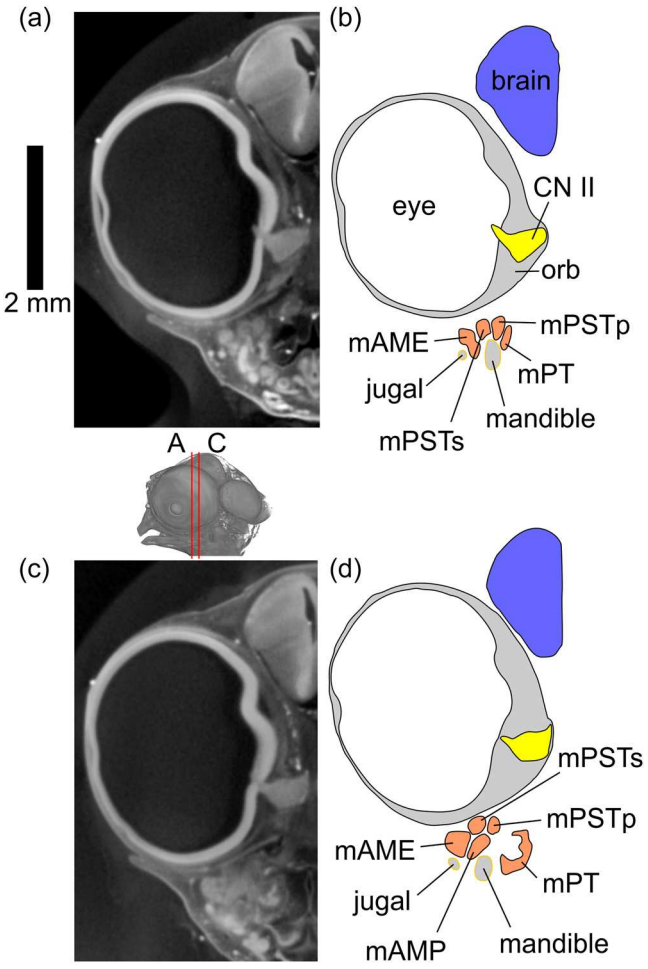

FIGURE 2 Serial diceCT slice images (a, c) and tracings (b, d) of cranial soft tissues in a chick at embryonic day 9. CN II, optic n; diceCT, iodine-based contrast-enhanced computed tomography; mAME, musculus adductor mandibulae externus; mAMP, musculus adductor mandibulae posterior; mPSTp, musculus pseudotemporalis profundus; mPSTs, musculus pseudotemporalis superficialis; mPT, musculus pterygoideus; orb, orbital soft tissues.

We tracked the component parts of this muscle group—mPSTs, mPSTp, and mPT—back to specimens as young as embryonic day 9 (Figure 2). McClearn and Noden (1988) distinguished these components in quail embryos at earlier time points, around days 6 and 7. However, we could not unequivocally distinguish between the dorsal and ventral pterygoid muscles (musculus pterygoideus dorsalis [mPTd] and musculus pterygoideus ventralis [mPTv], respectively) in specimens younger than embryonic day 18.

mPSTs is a relatively thin muscle that stretches from the rostral face of the rostrolateral laterosphenoid to the dorsomedial surface of the dentary. In specimens at embryonic day 9, mPSTs is cigar- or cord-shaped, slightly thicker at its midpoint than at the attachments (Figure 5). The proximal half of the muscle grows flatter in older specimens, and by embryonic day 18 the muscle is straplike proximally and tapers to a cord at its distal attachment on the mandible. In young specimens, mPSTs courses straight from its rostral

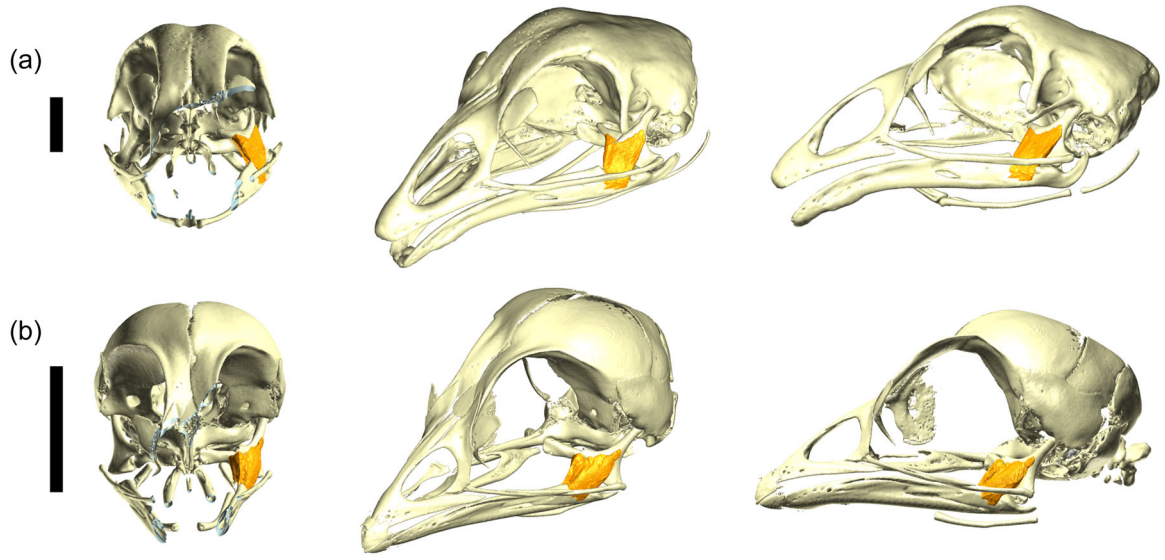

FIGURE 3 Musculus adductor mandibulae posterior (mAMP) in adult and hatchling *Gallus gallus*. In both figure portions, views from left to right are rostral, rostrolateral oblique, and lateral. (a) Adult chicken with mAMP and (b) hatchling chick with mAMP. Note that the muscle is more laterally oriented in the adult. Scalebars are both 10 mm.

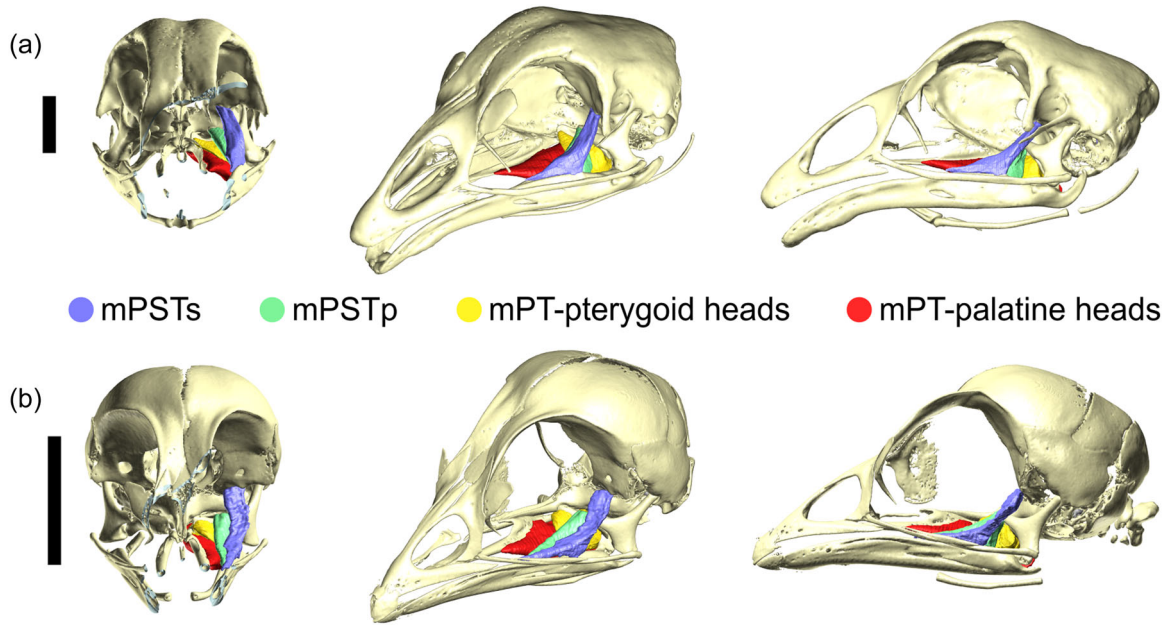

FIGURE 4 Musculus adductor mandibulae internus (mAMI) in adult and hatchling *Gallus gallus*. In both figure portions, views from left to right are rostral, rostrolateral oblique, and lateral. The components of mAMI in the figure are musculus pseudotemporalis superficialis (mPSTs, blue), musculus pseudotemporalis profundus (mPSTp, green), pterygoid heads of musculus pterygoideus (mPT, yellow), and palatine heads of musculus pterygoideus (mPT, red). (a) Adult chicken with the components of mAMI and (b) hatchling chick with the components of mAMI. Note that the mandible is laterally broader, relative to the braincase, in the adult than in the chick. The pseudotemporalis muscles in the adult are both more laterally oriented than those in the chick. Scalebars are both 10 mm.

attachment to its distal attachment, but by embryonic day 18 the muscle has developed a gentle curve paralleling the caudal contour of the eyeball. In postnatal specimens, the attachment of mPSTs to the dentary runs rostrally, just medial and parallel to the attachment of musculus adductor mandibulae externus profundus (mAMEP), and hugs the dorsomedial surface of the dentary for several millimeters.

Pseudotemporalis superficialis is consistently located just medial to mAME, just rostrodorsal to mAMP, and just lateral to mPSTp. The orientation of both pseudotemporalis muscles shifts during ontogeny in a similar way to mAMP. These muscles have more of a lateral component to their orientation in adult specimens than in young specimens (Figure 4).

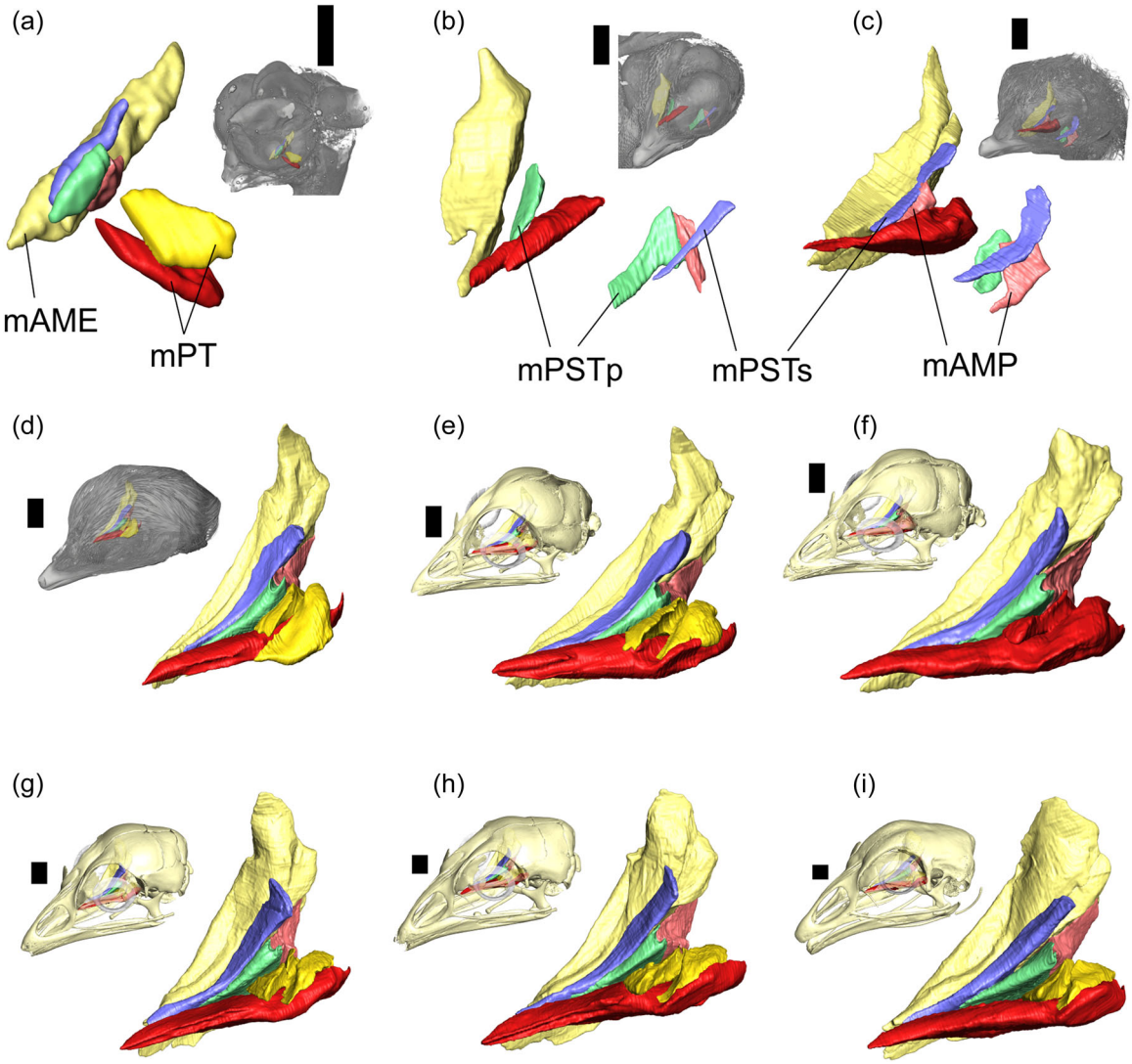

FIGURE 5 Rostrolateral oblique views of the jaw-adductor muscles across the sample. Insets show the location of the muscles within the head. Due to less mineralization of the embryos (a–d), these insets are volumes of the entire head rather than skulls. Scalebars are all 5 mm. (a) embryonic day 9, (b) embryonic day 12, (c) embryonic day 15, (d) embryonic day 18, (e) hatchling, (f) 1-week after hatching, (g) 3-weeks after hatching, (h) 6-weeks after hatching, and (i) adult. Note that at embryonic days 12 and 15, as well as in the specimen 1-week old, clear divisions between the pterygoid and palatine heads of the pterygoideus muscle were not identified, so the entire volume of the muscle was segmented as a unit. mAME; musculus adductor mandibulae externus; mAMP, musculus adductor mandibulae posterior; mPSTp, musculus pseudotemporalis profundus; mPSTs, musculus pseudotemporalis superficialis; mPT, musculus pterygoideus dorsalis.

mPSTp is a more robust wedge of muscle in the chick than mPSTs. The deep pseudotemporalis muscle stretches from the rostroventral surface of the medial-most aspect of the orbital process of the quadrate to the medial face of the dentary close to the inferior alveolar canal. In the diceCT data of older specimens, the mandibular division of the trigeminal nerve can be identified entering the inferior alveolar canal just lateral to mPSTp (Figure 6; see also Holliday & Witmer, 2007). At its medial attachment on the quadrate, mPSTp is nearly continuous with mAMP (Figure 5). These two muscles form a fan of muscle fibers spanning the space between the quadrate and the mandible. Whereas mAMP is a relatively short muscle, however, the rostral attachment of mPSTp is at nearly the same point on the dentary as the rostral-most point of mPSTs. The juxtaposition of mPSTp and mAMP may represent an intermuscular connection like those described by Elzanowski (1993), although that study did not identify interconnections between these two muscles.

Musculi pterygoidei dorsalis et ventralis stretch from the pterygoid and palatine bones to the mandible. There, the dorsal muscle mass inserts just ventral to the jaw joint. The ventral muscle mass inserts on the medial mandibular process, cupping its ventral surface. We first identified these muscles in CT data of specimens at embryonic day 9 (Figure 2). In these young specimens, the primordium of mPT is an undifferentiated mass of tissue caudal to the other muscle primordia of the adductor apparatus, though dorsal and ventral masses are detectable (Figure 5). By embryonic day 12, mPT sits medial to the other developing muscles and broadly

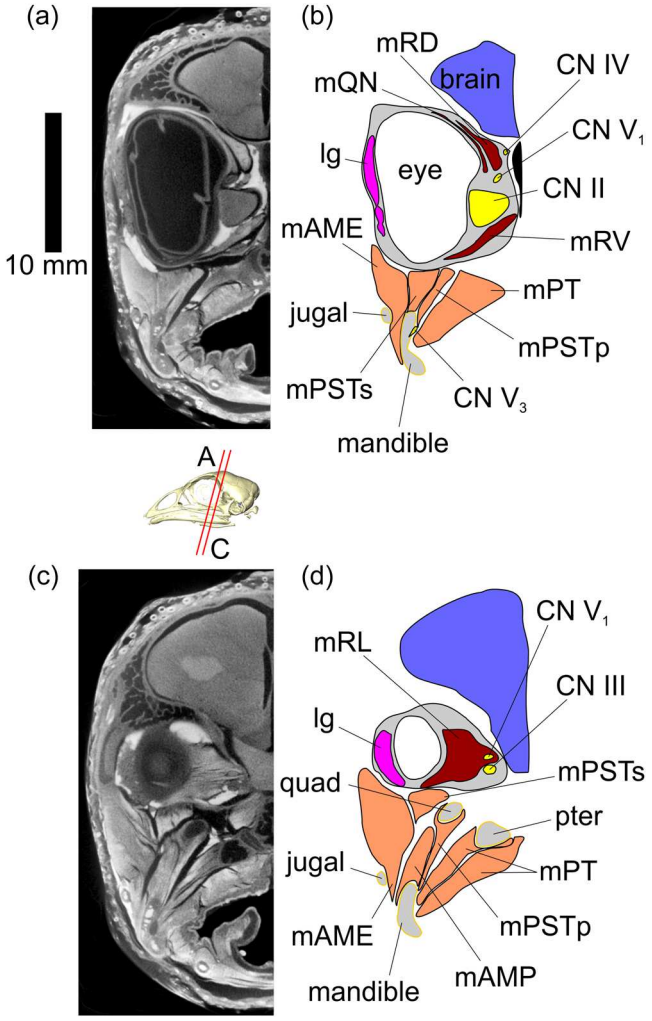

FIGURE 6 Serial diceCT slice images (a, c) and tracings (b, d) of cranial soft tissues in a chick 6 weeks old. CN II—optic n; CN III, oculomotor n; CN IV, trochlear n; CN V_1, ophthalmic division of trigeminal n; CN V_3, mandibular division of trigeminal n; diceCT, iodine-based contrast-enhanced computed tomography; lg, lacrimal gland; mAME, musculus adductor mandibulae externus; mAMP, musculus adductor mandibulae posterior; mPSTp, musculus pseudotemporalis profundus; mPSTs, musculus pseudotemporalis superficialis; mPT, musculus pterygoideus; mRD, musculus rectus dorsalis; mRL, rectus lateralis; mRV, musculus rectus ventralis; mQN, musculus quadratus membranae nictitantis; pter, pterygoid; quad, quadrate.

resembles its mature form: a long triangle of tissue flattened dorsoventrally, attached to the palatine, and capped dorsally by a smaller mass of tissue attached to the pterygoid (Figure 7). Although mPT is larger than the other components of mAMI in these embryos, mPT is still smaller than the mAME primordium. By embryonic day 18, however, mPTd and mPTv together just exceed the volume of mAME. The pterygoideus muscles together are always the largest adductor muscles by volume in specimens older than embryonic day 18.

In the diceCT data from our sample of chicks, separations between mPTd and mPTv are indistinct (Figure 8). The pterygoid heads of these muscles appear to be a single muscle originating from both the lateral and medial faces of the pterygoid bone. The palatine heads of the pterygoideus muscles similarly appear to be a single mass in the CT data. In reality, divisions between the two pterygoid muscles have been described with precision for both neognaths and paleognaths by Holliday and Witmer (2007) and appreciated at least since Edgeworth (1907), which distinguished two divisions of mPT in embryos of *Gallus* by the end of embryonic day 7.

3.1.3 | Musculus adductor mandibulae externus

This large muscle group is the most lateral and superficial of the three we studied. Adductor mandibulae externus is bounded laterally by the skin and medially by the mandible, mPSTs, and mAMP. Although mAME is generally composed of superficial, medial, and deep bellies in archosaurs, previous studies reported that the medial belly is not present in birds (Holliday & Witmer, 2007). Other recent work reported evidence of a medial belly in *G. gallus* itself and other modern birds (Cost et al., 2022; Holliday, 2009). In the CT data of our sample of *Gallus* embryos and chicks, the external jaw adductors appear to separate naturally into three masses. These masses can be consistently tracked across the developmental series, including in specimens as young as embryonic day 15. It is plausible that the separation between "medial," superficial, and deep muscle masses is artifactually enhanced by immersion in Lugol's iodine (Gignac et al., 2016), and indeed the separations between muscle masses are in some data sets quite subtle. Nonetheless, because the attachments of these masses in our sample match well with recent work (see Cost et al., 2022, for additional commentary on mAME in a comparative context), we track them as individual muscle bellies.

The superficial (mAMES), medial (mAMEM), and deep (mAMEP) bellies are distinguishable in CT data of chicks as young as embryonic day 15 (Figure 9). The superficial muscle belly extends from the lateral surface of the squamosal and dorsolateral surface of the otic process of the quadrate to the caudal half of a broad fossa on the lateral surface of the lower jaw just ventrolateral to the coronoid fossa. The medial belly attaches dorsally to the lateral surface of the squamosal, processus zygomaticus, and, in adults, the ventral tip of the processus postorbitalis. From there, mAMEM extends to the lateral face of the mandible, just dorsal to the fenestra rostralis mandibulae and rostral to the attachment of mAMES. The deep belly stretches from the dorsotemporal fossa (i.e., the lateral face of the squamosal between postorbital and zygomatic processes) to the dorsal and dorsolateral surfaces of the mandible. The mandibular attachment of mAMEP is quite long, stretching from the coronoid process to the dorsal surface of the mandible above the rostral mandibulae fenestra.

The form of this muscle differs only slightly between younger and older specimens (Figure 10). At embryonic day 9, the mAME primordia are a strap extending straight from the temporal region to

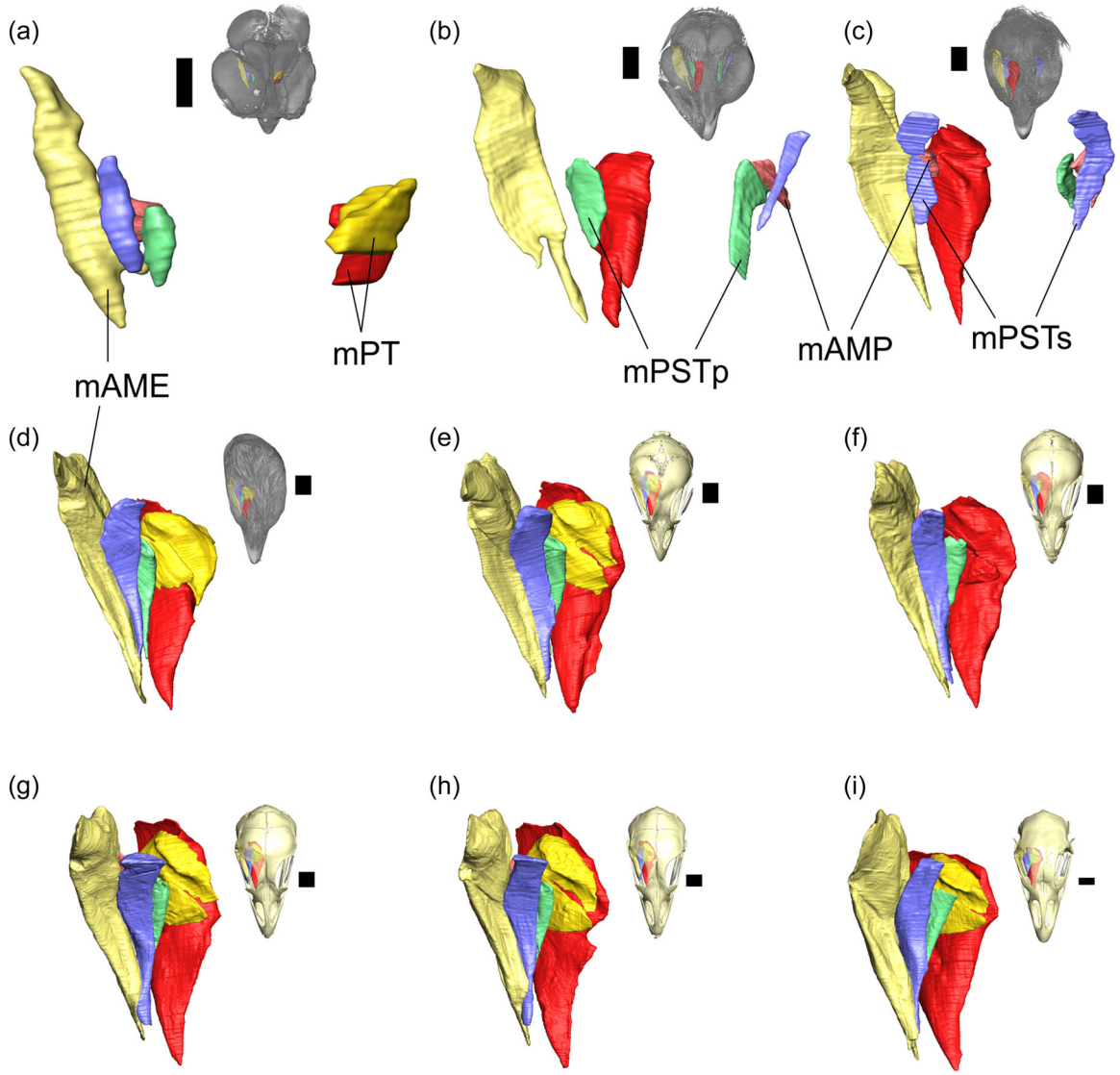

FIGURE 7 Dorsal views of the jaw-adductor muscles across the sample. Insets show the location of the muscles within the head. Due to less mineralization of the embryos (a–d), these insets are volumes of the entire head rather than skulls. Scalebars are all 5 mm. (a) Embryonic day 9, (b) embryonic day 12, (c) embryonic day 15, (d) embryonic day 18, (e) hatchling, (f) 1-week after hatching, (g) 3-weeks after hatching, (h) 6-weeks after hatching, and (i) adult. Note that at embryonic days 12 and 15, as well as in the specimen 1-week old, clear divisions between the pterygoid and palatine heads of the pterygoideus muscle were not identified, so the entire volume of the muscle was segmented as a unit. mAME; musculus adductor mandibulae externus; mAMP, musculus adductor mandibulae posterior; mPSTp, musculus pseudotemporalis profundus; mPSTs, musculus pseudotemporalis superficialis; mPT, musculus pterygoideus dorsalis.

the lower jaw. Though wide, the strap of mAME is much smaller than, for example, the nearby extraocular muscles. The muscle strap tapers to points at its proximal and distal attachments. By the perinatal period (embryonic days 18–21), the pterygoideus muscles are larger than mAME. The dorsal attachment of mAME is cigar-shaped and occupies a small bony fossa. The muscle is widest at its midpoint, but its ventral attachment has begun to spread out along the mandible. The muscle has also begun to take on a gentle curve whereby the muscle fibers first extend ventrally from the temporal region and then turn rostroventrally around the developing postorbital process to reach the dentary.

These changes are successively more pronounced in older specimens. In the adults, the postorbital process is so long that the body of mAME is indented by the bone where the two structures are in contact. Furthermore, the dorsal temporal fenestra is most pronounced (i.e., most deeply carved out) in older specimens. The dorsal and ventral attachments of mAME are as wide or wider than the midpoints of the muscle bellies. Indeed, the dorsal attachment of mAMEP in the adults covers the caudal half of the lateral face of the postorbital process for its entire length. Finally, whereas mAME has a significant medial component to its orientation in younger specimens, the muscle is oriented predominantly rostroventrally in adults (Figure 10).

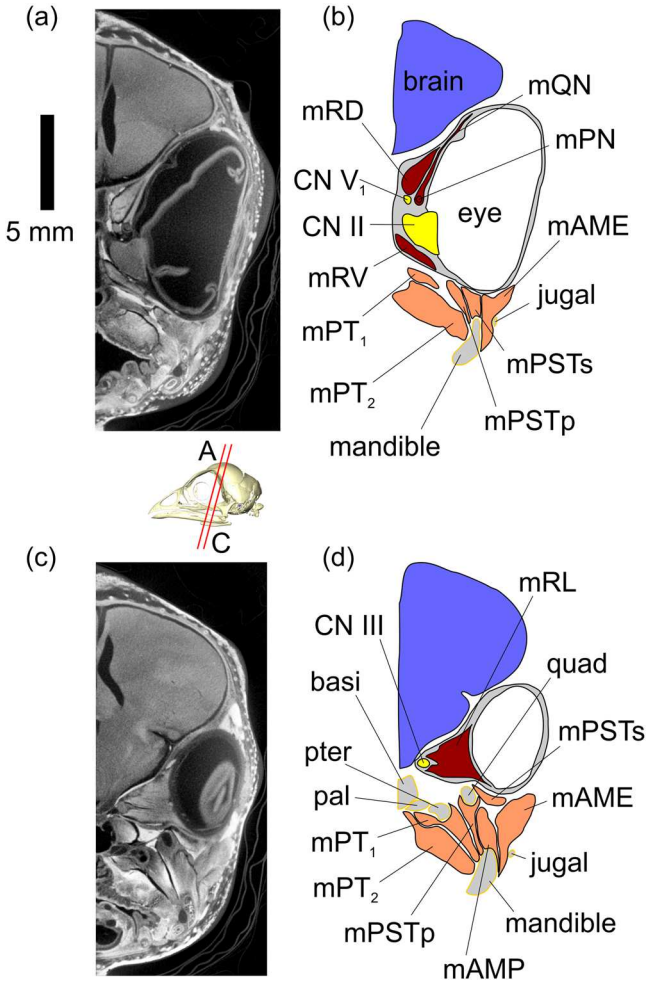

FIGURE 8 Serial diceCT slice images (a, c) and tracings (b, d) of cranial soft tissues in a hatchling chick, with a focus on the pterygoid and palatine masses of musculus pterygoideus. basi, basisphenoid; CN II, optic n; CN III, oculomotor n; CN V_1, ophthalmic division of trigeminal n; diceCT, iodine-based contrast-enhanced computed tomography; mAME, musculus adductor mandibulae externus; mAMP, musculus adductor mandibulae posterior; mPN, musculus tendon of pyramidalis membranae nictitantis; mPSTp, musculus pseudotemporalis profundus; mPSTs, musculus pseudotemporalis superficialis; mPT_1, musculus pterygoid heads of pterygoideus; mPT_2, musculus palatine heads of pterygoideus; mRD, musculus rectus dorsalis; mRL, musculus rectus lateralis; mRV, musculus rectus ventralis; mQN, musculus quadratus membranae nictitantis; pal, palatine; pter, pterygoid; quad, quadrate.

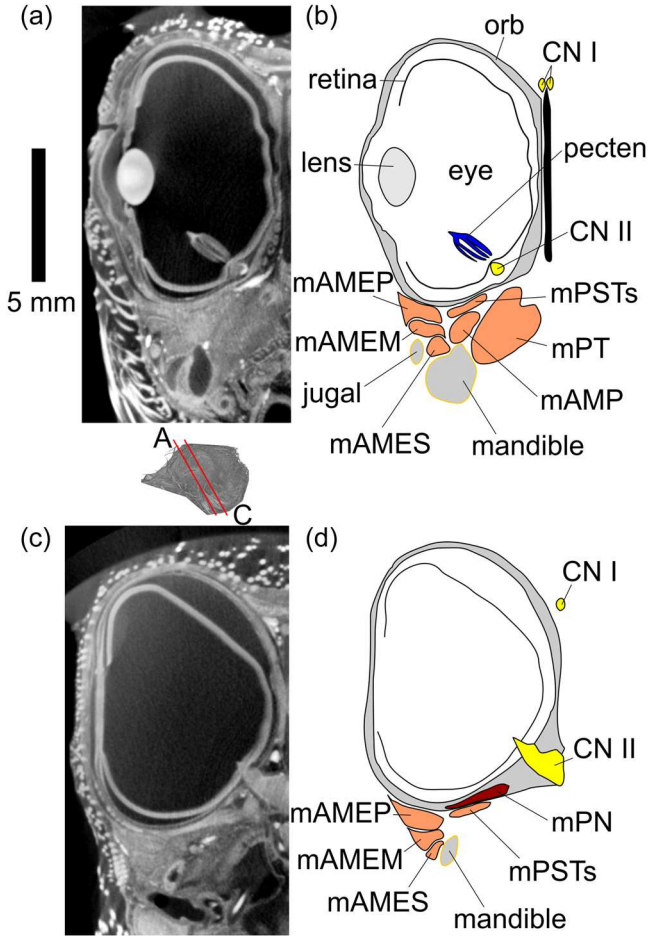

FIGURE 9 Serial diceCT slice images (a, c) and tracings (b, d) of cranial soft tissues in a chick at embryonic day 15, with a focus on the bellies of musculus adductor mandibulae externus. CN I, olfactory n; CN II, optic n; diceCT, iodine-based contrast-enhanced computed tomography; mAMEM, musculus adductor mandibulae externus medialis; mAMEP, musculus adductor mandibulae externus profundus; mAMES, musculus adductor mandibulae externus superficialis; mAMP, musculus adductor mandibulae posterior; mPN, musculus pyramidalis membranae nictitantis; mPSTs, musculus pseudotemporalis superficialis; mPT, musculus pterygoideus; orb, orbital soft tissues.

3.2 | Qualitative assessment of the bony adductor chamber over ontogenetic time

The anatomy of the bony adductor chamber is fairly constant over the course of development, but there are some notable changes to the laterosphenoid, quadrate, and palatine bones (Figure 11). The most significant osteological change is at the fossa for mAME (dorsal temporal fossa), located just rostrodorsal to the otic process of the quadrate. In Galliformes, this fossa is formed by the postorbital process of the laterosphenoid and the squamosal (Baumel & Witmer, 1993). At hatching (embryonic day 21), this fossa is shallow, subtle, and approximately semicircular in lateral view. The fossa is made up mostly of the lateral surface of the laterosphenoid, and the edges of the fossa are indistinct. Furthermore, the postorbital process—which delimits the fossa for mAME rostrally—is incompletely ossified at hatching, so the process is not visible in dorsal view when observing the skull without soft tissues. By the third-week after hatching, the fossa for mAME expands dorsally such that it resembles half of an ovoid, rather than a semicircle, in lateral view. The squamosal contributes more to the fossa. The dorsal edge of the fossa is more distinct, though no ridge or process clearly delimits it. The postorbital process has completed its ossification and protrudes laterally from the skull in dorsal view. Between the 6th- and 35th-week after hatching, the fossa for mAME has continued its dorsal

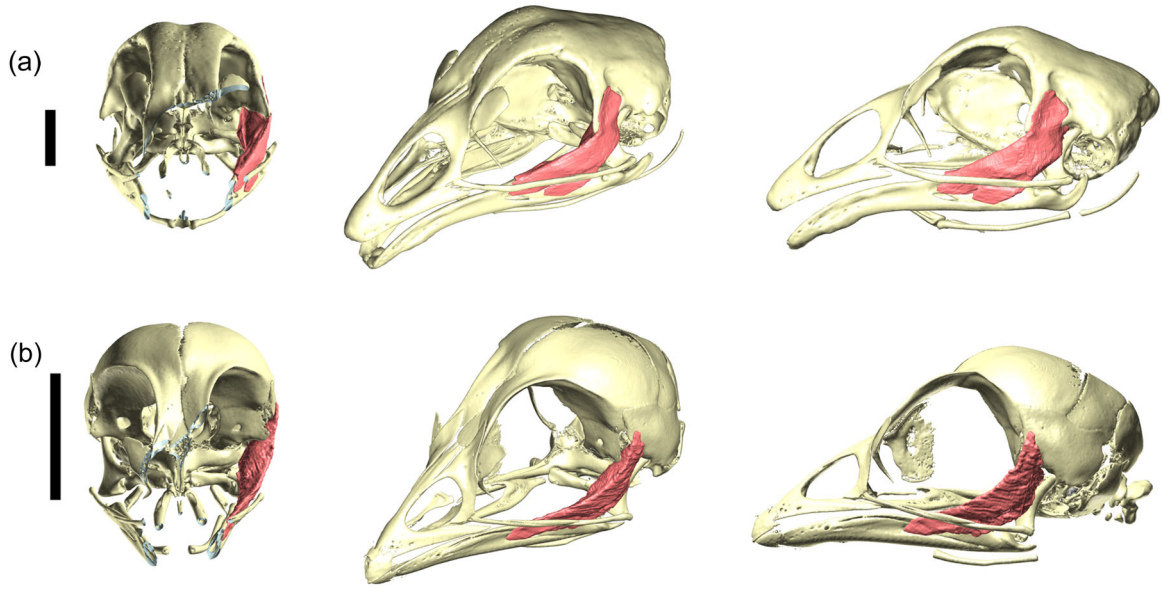

FIGURE 10 Musculus adductor mandibulae externus (mAME) in adult and hatchling *Gallus gallus*. In both figure portions, views from left to right are rostral, rostrolateral oblique, and lateral. (a) Adult chicken with mAME and (b) hatchling chick with mAME. Note that the dorsal attachments of the muscle have expanded laterally in the adult, allowing the muscle to have a predominantly rostroventral orientation with less medial deviation than in the chick. Scalebars are both 10 mm.

expansion such that it is subtriangular. The rostrodorsal, dorsal, and caudodorsal edges of the fossa are capped by a low-but-sharp ridge. The postorbital process protrudes laterally about 2.5 mm from the skull in dorsal view.

The next most-pronounced osteological changes to the adductor chamber are in the palatine and the quadrate. The lateral edge of the palatine is the medial attachment of mPTv. At hatching, this edge of the palatine is rounded and blunt, but it gradually thins into a wing-like lateral extension of the bone in progressively older specimens. The quadrate becomes more robust from hatching onwards. The orbital process of the quadrate, in particular, develops a more pronounced caudomedial curve relative to the body of the quadrate. At hatching, the orbital process is primarily oriented straight medially. By the 35th-week after hatching, the orbital process begins to curve much more strongly at a low vertical ridge found at the transition between the body and the orbital process. This ridge, which indicates the separation between the attachment sites of mAMP and mPSTp, only becomes apparent between the 6th- and 35th-week after hatching (Figure 11).

3.3 | Size analysis

3.3.1 | Change in size over time

The brain and the jaw muscles exhibit different patterns of growth over time (Figure 12a). The raw volume of the brain grows quickly, approximating a logarithmic curve in which growth begins to flatten around the third-week after hatching (~42 days). The raw volume of the jaw adductors grows steadily but comparatively slowly, approximating a linear curve that only appears to flatten sometime after the 6th-week post-hatching (~63 days). In absolute terms, the jaw adductors add about 8.89 mm^3 of volume per day of development during those first 63 days ($p < .001$, $r^2 = 0.968$). Of the three broad muscle groups, mAMI grows most quickly during this period at about 4.90 mm^3/day ($p < .001$, $r^2 = 0.967$). Adductor mandibulae externus grows only slightly slower at about 3.36 mm^3/day ($p < .001$, $r^2 = 0.962$). Adductor mandibulae posterior grows the slowest at about 0.622 mm^3/day ($p < .001$, $r^2 = 0.972$). Each muscle group grows at an approximately linear rate with respect to time for the first 63 days.

The growth of the eyes, like the brain, approximates a logarithmic curve in which growth begins to flatten around the third-week after hatching (Figure 12b). Eyes appear to grow even faster than the brain before and after hatching. In contrast to the brain, however, the eyes of embryos in the perinatal period (specifically, at 18 and 21 days) are essentially equal in size, indicating an arrest or minimally a slowing of growth around hatching.

3.3.2 | Brain-adductor allometry

The log-transformed volume of the jaw-adductor musculature grows with positive allometry relative to the log-transformed volume of the brain (Figure 13a). This relationship is different from isometry ($p < .001$), and it holds true when considering the total volume of the adductor complex (Table 2) and of each group of muscles, mAME, mAMI, and mAMP (Figure 13b). The slopes of these relationships for mAME, mAMI, and mAMP are not different from each other ($p = .177$, $F = 1.79$, sum of squares = 0.0327). Allometric slopes for individual muscles (mAMEM = 1.72, mAMEP = 1.35, mAMES = 1.56,

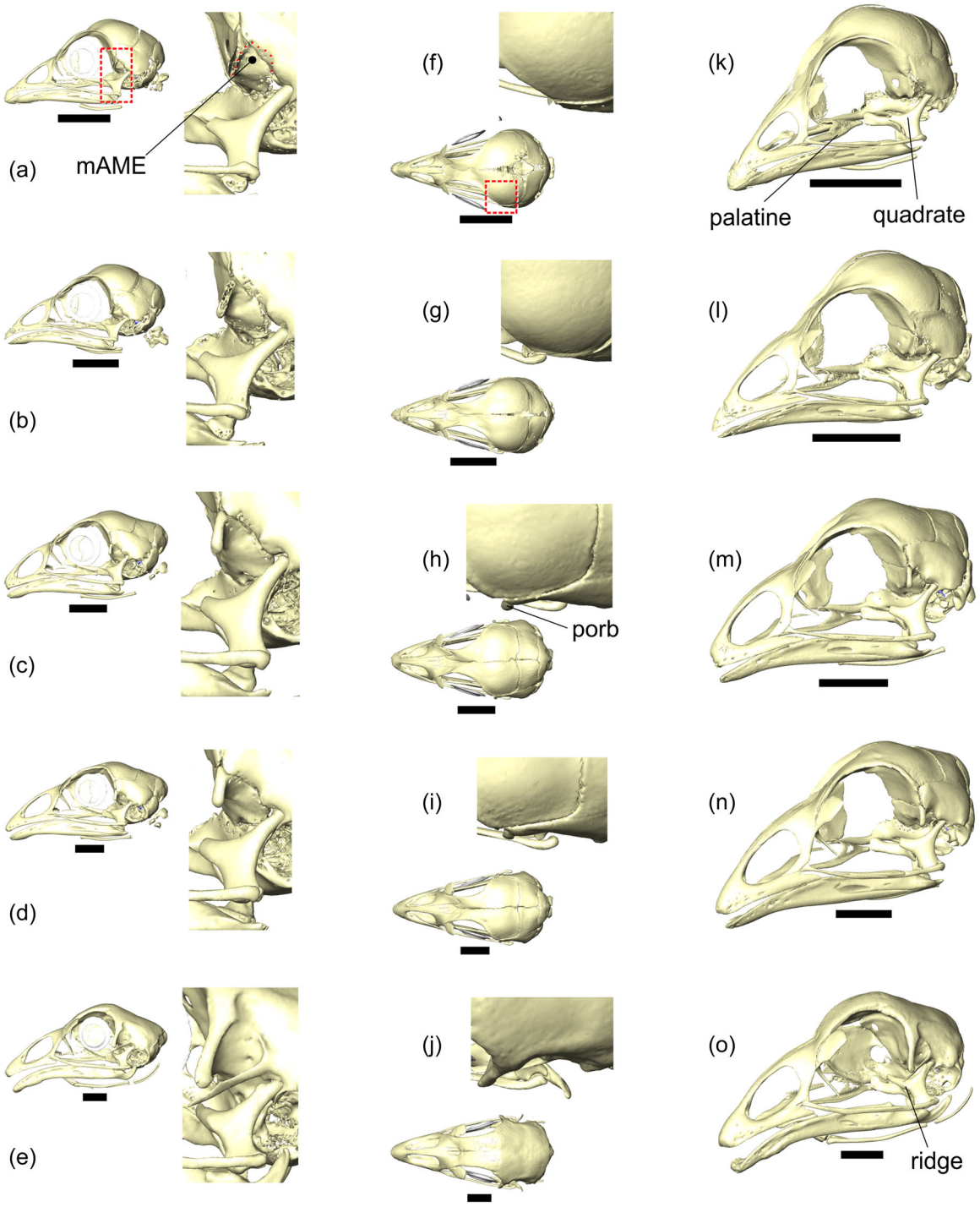

FIGURE 11 Osteology of the jaw-adductor chamber in *Gallus gallus* across post-hatching ontogeny. The skull of hatchling (a, f, k), 1-week old (b, g, l), 3-weeks old (c, h, m), 6-weeks old (d, i, n), and adult (e, j, o) chickens is presented in lateral (a–e), dorsal (f–j), and rostrolateral oblique views (k–o). The embayment for mAME elongates vertically in older specimens as the postorbital process grows and mineralizes. This process is visible in dorsal view by 3-weeks after hatching (h). The lateral margin of the palatine bone is blunt at hatching and becomes a thin wing in older specimens (k–o). The orbital process of the quadrate also grows and mineralizes over this time, until a subtle vertical ridge is apparent between this process and the body of the quadrate (o). Scalebars are all 10 mm. mAME, musculus adductor mandibulae externus dorsal attachment; porb, postorbital process.

mPT = 1.90, mPSTp = 1.88, mPSTs = 2.00, and mAMP = 2.01) cluster roughly around 1.70 (Figure 13c).

The jaw adductors grow with positive allometry relative to the size of the head (Figure 14), accounting for the different dimensions of these measurements. The brain, on the other hand, grows with negative allometry relative to the size of the head (Figure 15), accounting for the same difference in dimensions. Both relationships are distinguishable from isometry (p_{muscle} < .001; p_{brain} < .001). If the influence of head size is held constant and partial regressions are estimated between relative brain size and relative jaw-adductor size, two different trends are recovered depending on the metric of head size (Table 3 and Figure 16). If soft tissues are scaled to the width of the head at the quadrates (interquadrate distance), an inverse relationship is recovered between relative brain size and relative jaw-adductor size (p = .0427, t = −2.19) such that individuals with smaller brains than expected have larger jaw muscles than expected.

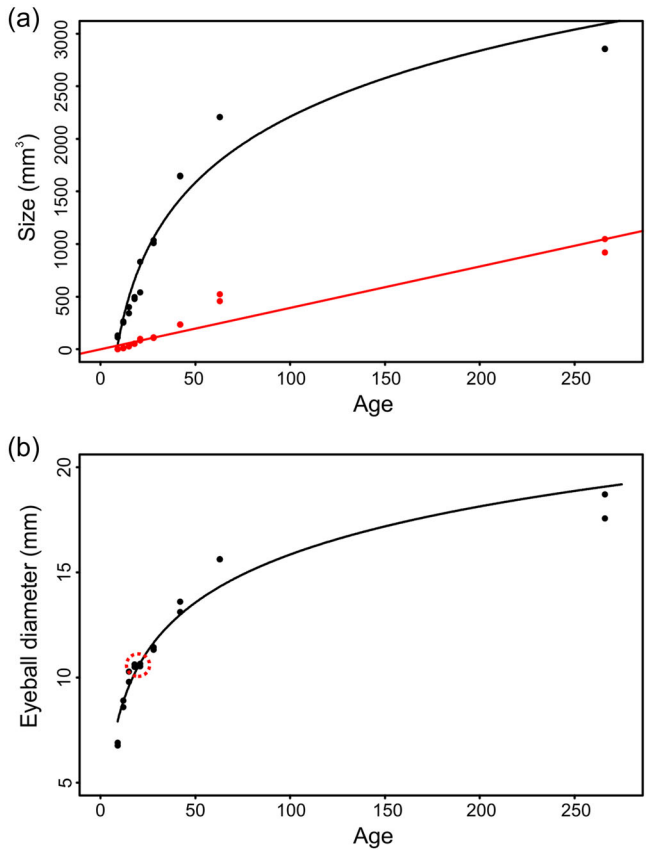

FIGURE 12 Growth curves of organ size versus age of specimens. Each time point (except embryonic days 5 and 6, at which measurements were not made; see Section 2) is represented by two specimens. Some pairs of specimens had nearly identical brain, muscle, or eye sizes, so there are some ages for which the plots appear to show only a single datapoint even though both specimens are represented on the plot. (a) Plot of brain volume and total volume of jaw adductors versus age. Black dots indicate brain volumes. Red dots indicate muscle volumes. (b) Plot of equatorial diameter of the eyeball versus age of specimens. The red dashed circle indicates the period of time (perinatal) when the eyes were essentially identical in size for specimens that differed by a full 3 days in age (embryonic days 18 and 21).

However, this regression explains little variance (r^2 = 0.174). A regression estimated using RMA yields a sharper slope but similarly poor explanatory power (p = .0449, r^2 = 0.216). The direction of this relationship is the same for mAMI (slope = −1.08, p = .0386, r^2 = 0.182, t = −2.24) and mAMP (slope = −1.71, p = .0427, r^2 = 0.174, t = −2.19), whereas no correlation is recovered for mAME (p = .221, t = −1.27). No difference among muscle groups is found (p = .697, F = 0.363, sum of squares = 0.00013). If soft tissues are scaled to the length of the braincase, relative brain size, and relative jaw-adductor size are clearly correlated with each other (p = .00187, r^2 = 0.410, t = 3.67) such that individuals with larger brains

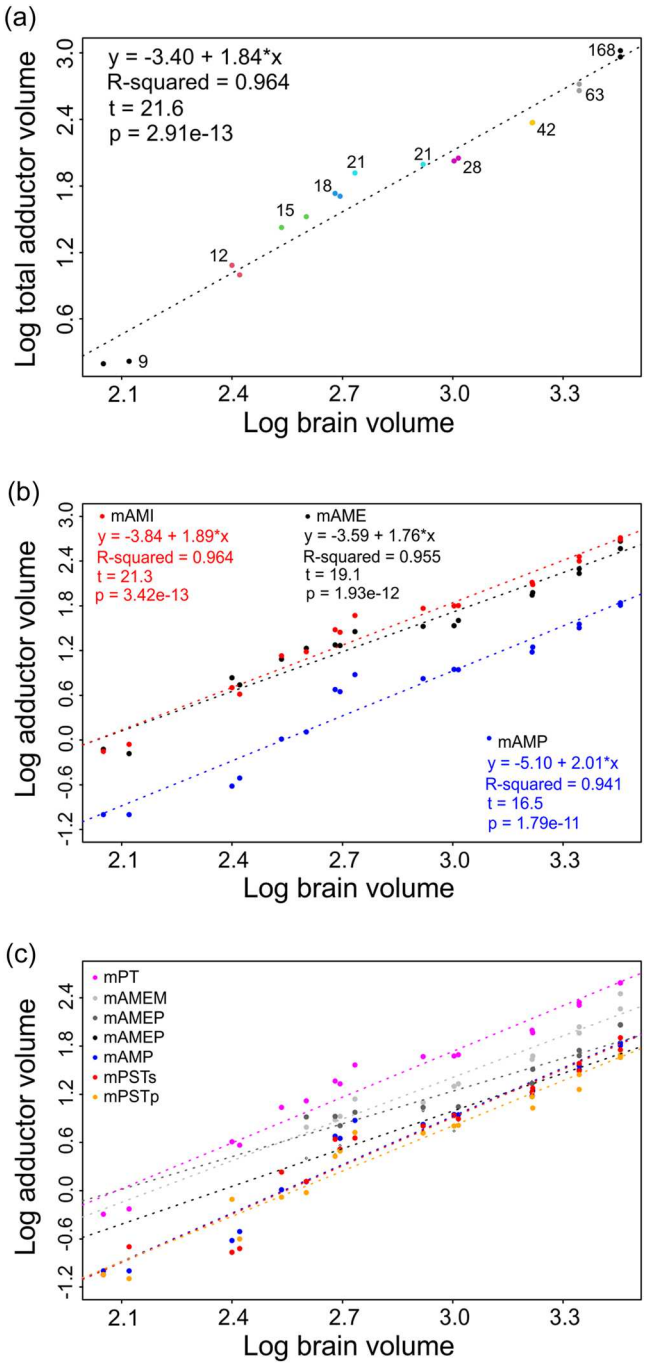

FIGURE 13 (See caption on next page).

than expected also have larger jaw muscles than expected. Results from RMA regression are similar ($p = .00171$, $r^2 = 0.448$). The direction of this relationship is the same for each group of jaw muscles: mAME (slope = 0.875, $p = .0122$, $r^2 = 0.275$, $t = 2.80$), mAMI (slope = 1.28, $p = .00132$, $r^2 = 0.432$, $t = 3.83$), and mAMP (slope = 1.37, $p = .0107$, $r^2 = 0.285$, $t = 2.86$). No difference among the groups is found ($p = .415$, $F = 0.894$, sum of squares = 0.00135).

3.3.3 | Eyeball-adductor allometry

The log-transformed volume of the jaw-adductor musculature grows with positive allometry relative to the log-transformed diameter of the eyeball (Figure 17a). This relationship is different from isometry ($p < .001$), and it holds true when considering the total volume of the adductor complex (Table 2) and of each group of muscles, mAME, mAMI, and mAMP (Figure 17b). The slopes of these relationships for mAME, mAMI, and mAMP are not different from each other ($p = .166$, $F = 1.86$, sum of squares = 0.0035). Allometric slopes for individual muscles (mAMEM = 1.93, mAMEP = 1.59, mAMES = 1.70, mPT = 2.22, mPSTp = 2.18, mPSTs = 2.33, and mAMP = 2.33) cluster roughly around 2 (Figure 17c).

The eyeball grows with negative allometry relative to the size of the head (Figure 18), and this relationship is distinguishable from isometry ($p < .001$). If the influence of head size is held constant and partial regressions are estimated between relative eyeball size and relative jaw-adductor size, similar trends are found regardless of the metric of head size (Figure 19). If soft tissues are scaled to the width of the head at the quadrates (interquadrate distance), no clear relationship is recovered ($p = .6432$, $t = 0.472$). If soft tissues are scaled to the length of the braincase, no clear relationship is recovered ($p = .128$, $t = 1.6$).

Despite the absence of a clear allometric relationship across the whole ontogenetic series, jaw adductors are generally small after hatching. This trend is more consistent in older specimens, regardless of whether eyes are relatively large or small. On the other hand, on the day of hatching and up to about a week before and after hatching, specimens have jaw adductors that are consistently large at a time when eyeballs are relatively small.

3.3.4 | Eyeball-brain allometry

The log-transformed diameter of the eyeball grows with negative allometry relative to the log-transformed volume of the brain (Table 2 and Figure 20), and this relationship is statistically distinguishable from isometry ($p = .00162$). If the influence of head size is held constant and partial regressions are estimated between relative brain size and relative eye size, there is no clear relationship (Table 3 and Figure 21) regardless of scaling to interquadrate distance or to braincase length. Notably, however, eyes are generally smaller than expected relative to interquadrate distance during the period between hatching and the third-week after hatching, at a time when brains are larger than expected (i.e., growing quickly).

4 | DISCUSSION

Here, we present a study of the qualitative and quantitative changes in jaw-adductor musculature, relative to the size of the brain and eyeballs, in an ontogenetic series of the domestic chicken *G. gallus*. Our overall objective was to quantitatively assess whether there are ontogenetic signatures of constructional constraints (Barel, 1982) imposed by the chick brain and eyeballs on the jaw-adductor musculature or vice versa. We aimed to measure how the adductor chamber changes during development, to model the strength of the putative allometric relationships between the two neurosensory organs and the jaw muscles, and to make a descriptive record of changes in muscle form over ontogenetic time. Authors have used histochemistry to shed light on the developmental origins of tissues in the avian cranium (e.g., van der Meij & Bout, 2004); others tracked morphological changes in the avian brain over development (Watanabe et al., 2019); and still others used diceCT to follow cranial nerves (Lessner & Holliday, 2020) and muscle orientation (Cost et al., 2022) through development in the sister group to birds (i.e., crocodylians). Our study is the first to use diceCT to quantitatively and qualitatively track the jaw adductors in a bird species through development. Moreover, we collected these data in the chick, an important model organism in disciplines from genomics to craniofacial development (Burt, 2007; Kiecker, 2016; Stern, 2005), adding to the robust body of work done on this system.

FIGURE 13 Plots of brain size versus jaw-adductor size, showing that jaw muscles grow with positive allometry relative to the brain. (a) Plot of brain volume versus total adductor volume. Labels correspond to age, as follows: embryonic day 21 corresponds to the day of hatching, day 28 to 1-week after hatching, day 42 to 3-weeks after hatching, and so forth. Datapoints in this figure portion are colored only to differentiate ages from each other. (b) Plot of brain volume versus the size of the three jaw-adductor groups, mAME (black), mAMI (red), and mAMP (blue). (c) Plot of brain volume versus the individual jaw muscles we tracked, mAMEM (light gray), mAMEP (dark gray), mAMES (black), mAMP (blue), mPSTp (gold), mPSTs (red), and mPT (magenta). Note that the three components of mAME were not unequivocally separable in any of the specimens at embryonic days 9 and 12, nor in one specimen at embryonic day 15, so the regression lines for mAMEM, mAMEP, and mAMES were estimated with 13 datapoints rather than the full 18. mAME; musculus adductor mandibulae externus; mAMEM, musculus adductor mandibulae externus medialis; mAMEP, musculus adductor mandibulae externus profundus; mAMES, musculus adductor mandibulae externus superficialis; mAMI, musculus adductor mandibulae internus; mAMP, musculus adductor mandibulae posterior; mPSTp, musculus pseudotemporalis profundus; mPSTs, musculus pseudotemporalis superficialis; mPT, musculus pterygoideus dorsalis.

TABLE 2 Summary of results from regression analyses using dimensions uncorrected for head size.

			OLS		RMA	
Variable 1	**Variable 2**	r^2	**Slope (95% CI)**	***p***	**Slope (95% CI)**	***p***
Brain	Eyeball	0.952	0.824 (0.726, 0.922)	<.001	0.845 (0.752, 0.949)	<.001
	Total muscle	0.966	1.84 (1.66, 2.02)	<.001	1.87 (1.70, 2.06)	<.001
	mAME	0.958	1.76 (1.57, 1.96)	<.001	1.80 (1.62, 2.01)	<.001
	mAMI	0.966	1.89 (1.70, 2.08)	<.001	1.92 (1.74, 2.12)	<.001
	mAMP	0.944	2.01 (1.75, 2.26)	<.001	2.06 (1.82, 2.34)	<.001
Eyeball	Total muscle	0.959	2.17 (1.93, 2.40)	<.001	2.21 (1.99, 2.46)	<.001
	mAME	0.971	2.10 (1.91, 2.29)	<.001	2.13 (1.95, 2.33)	<.001
	mAMI	0.946	2.22 (1.94, 2.49)	<.001	2.28 (2.01, 2.57)	<.001
	mAMP	0.911	2.33 (1.95, 2.72)	<.001	2.44 (2.09, 2.86)	<.001

Abbreviations: CI, confidence interval; mAME, musculus adductor mandibulae externus; mAMI, musculus adductor mandibulae internus; mAMP, musculus adductor mandibulae posterior; OLS, ordinary least-squares regression; RMA, reduced major axis regression.

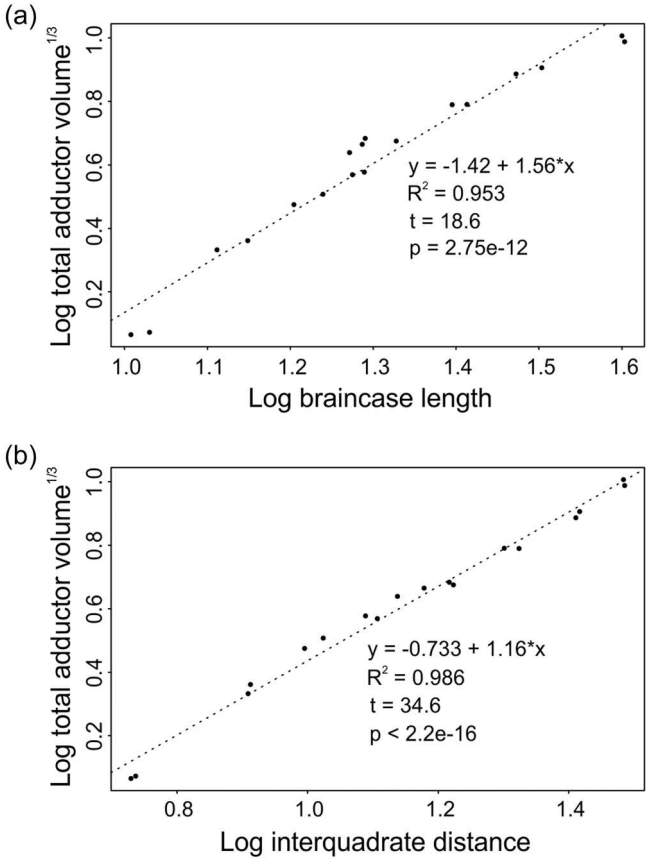

FIGURE 14 Plots of two measures of head size versus jaw-adductor volume. The cube root of muscle volume was taken before log transformation. (a) Length of the braincase versus volume of jaw-adductor muscles and (b) head width (interquadrate distance) versus volume of jaw-adductor muscles.

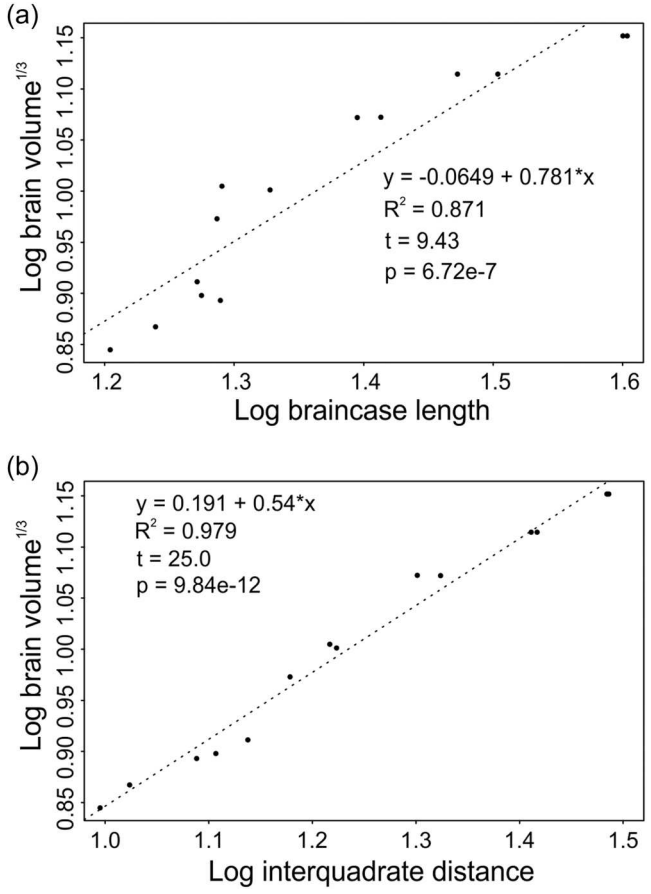

FIGURE 15 Plots of two measures of head size versus brain volume. The cube root of brain volume was taken before log transformation. (a) Length of the braincase versus brain volume and (b) head width (interquadrate distance) versus brain volume.

TABLE 3 Summary of results from regression analyses using dimensions relative to head size.

			OLS			RMA		
Variable 1	**Variable 2**	**Relative to**	**Slope (95% CI)**	r^2	***p***	**Slope (95% CI)**	r^2	***p***
Brain	Muscle	Interquadrate distance	−1.02 (−2.03, −0.00211)	0.174	.0427	−2.17 (−3.37, −1.40)	0.216	.0449
		Braincase length	1.11 (0.452, 1.77)	0.410	.00187	1.67 (1.14, 2.45)	0.448	.00171
	Eyeball	Interquadrate distance	−0.283 (−1.08, 0.517)	0.0340	.449	−1.54 (−2.50, −0.950)	0.0321	.462
		Braincase length	0.170 (−0.0499, 0.391)	0.0935	.109	0.447 (0.283, 0.706)	0.146	.105
Eyeball	Muscle	Interquadrate distance	0.160 (−0.584, 0.905)	0.0129	.653	1.41 (0.865-2.30)	0.0139	.629
		Braincase length	1.34 (−0.493, 3.18)	0.130	.140	3.74 (2.36, 5.92)	0.133	.123

Abbreviations: CI, confidence interval; OLS, ordinary least-squares regression; RMA, reduced major axis regression.

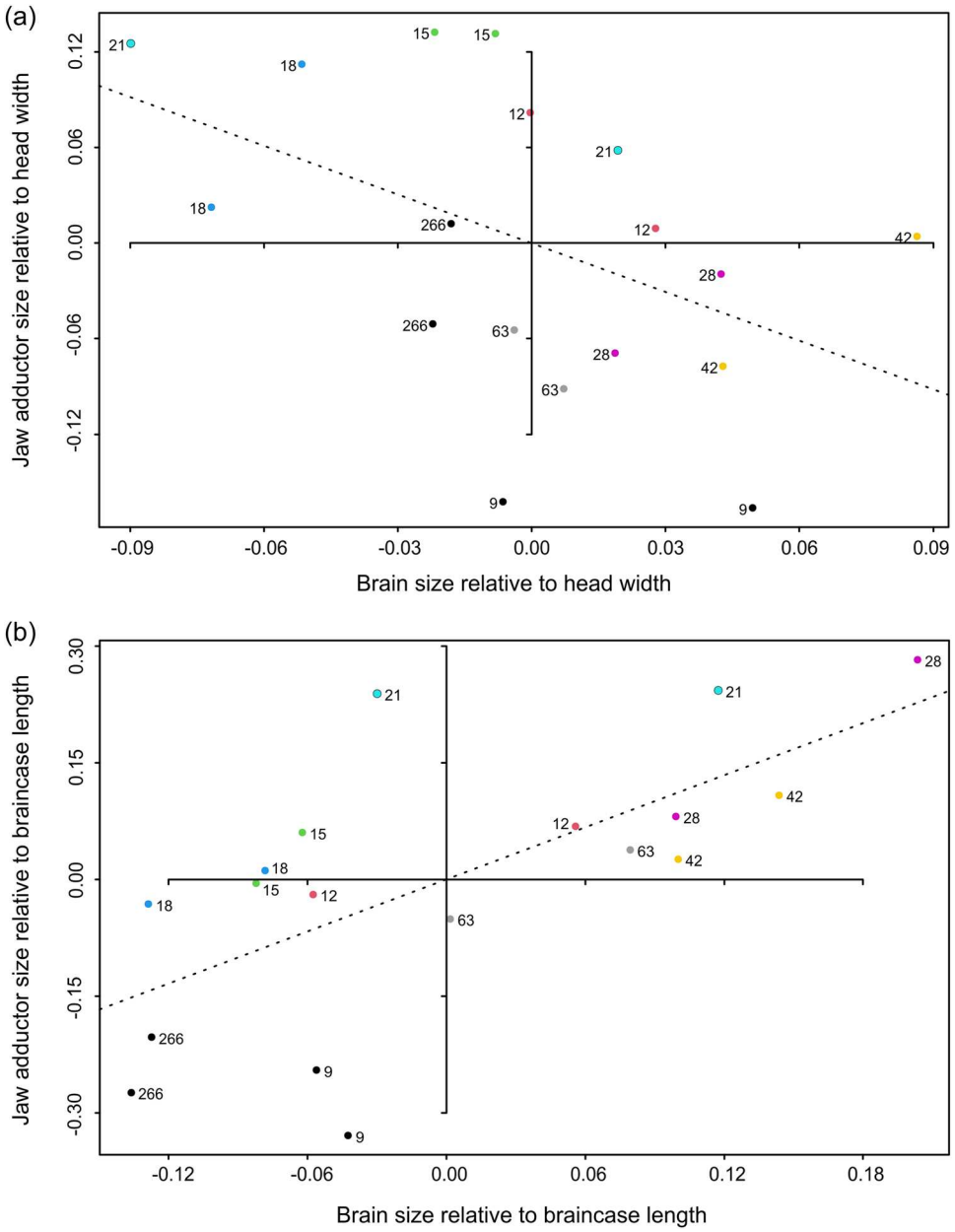

FIGURE 16 Plots of brain size versus jaw muscle size, with both dimensions relative to a linear dimension of the skull. (a) Here, sizes of soft tissues are relative to interquadrate distance. A clear, but weak, inverse relationship was recovered between these variables. Specimens with smaller-than-expected brains had larger-than-expected jaw muscles, coinciding roughly with specimens between embryonic days 15 and 21. (b) Plot of brain size versus jaw muscle size, with both dimensions relative to the length of the braincase. Clear evidence of a direct relationship between these variables was recovered, such that specimens with larger-than-expected brains also had larger-than-expected jaw muscles.

4.1 | Growth of the jaw adductors

The jaw-adductor musculature grows differently than the brain, which expands quickly both before hatching and in the perinatal period but begins to level off in its growth around the third-week after hatching. Our observations on brain size comport with past work that found brains develop quickly before hatching and slowly after hatching in precocial birds like *Gallus*, whereas more altricial species show the opposite pattern (Bennett & Harvey, 1985). In contrast, we found that the jaw muscles grow relatively steadily through time. These muscles grow slower than the brain before hatching but at a similar rate after hatching, leveling off in their

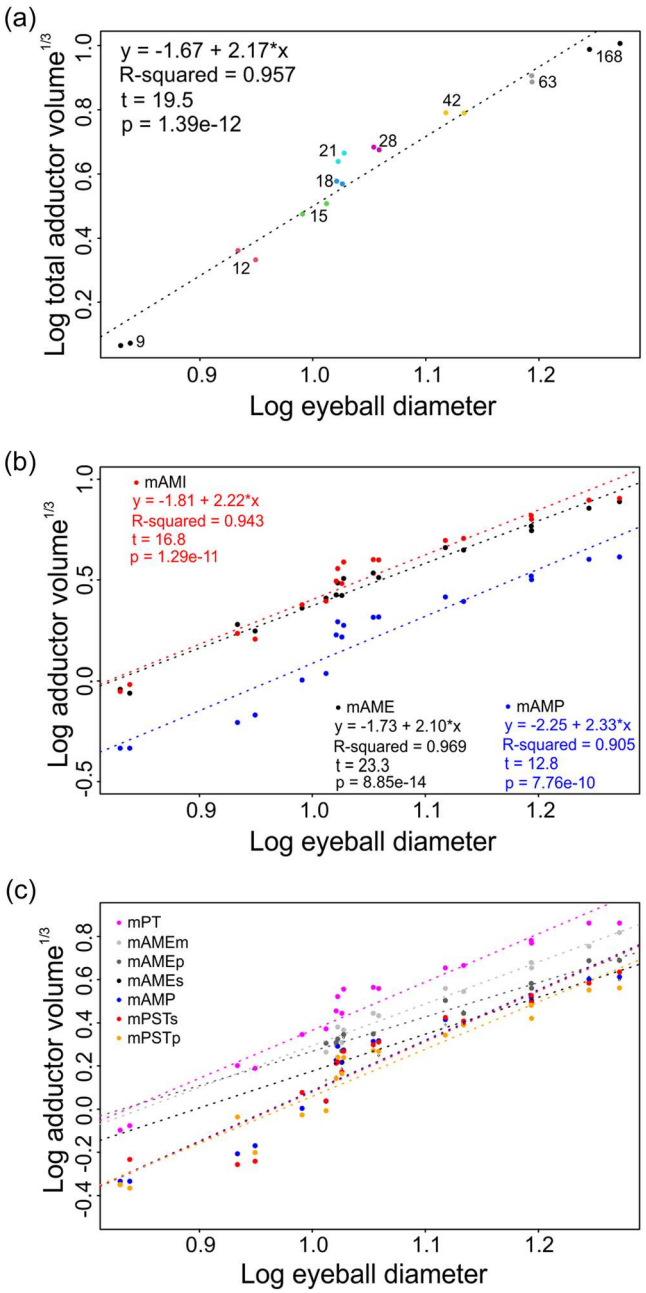

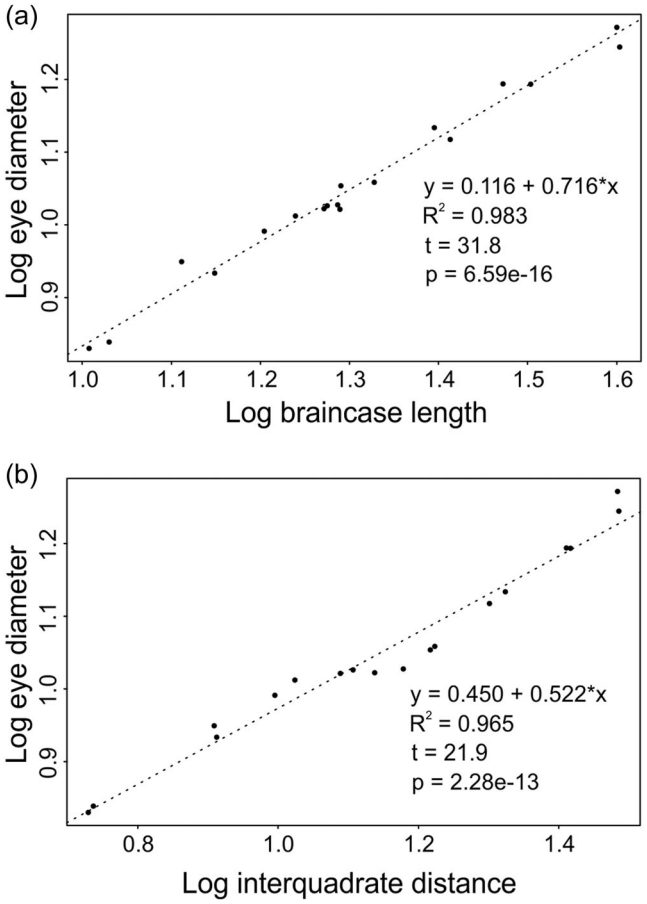

FIGURE 18 Plots of two measures of head size versus eyeball diameter. (a) Length of the braincase versus eyeball diameter and (b) head width (interquadrate distance) versus eyeball diameter.

FIGURE 17 Plots of eye size versus jaw-adductor size, showing that jaw muscles grow with positive allometry relative to the eyeball. (a) Plot of eyeball diameter versus total adductor volume. Labels correspond to age, as follows: embryonic day 21 corresponds to the day of hatching, day 28 to 1-week after hatching, day 42 to 3-weeks after hatching, and so forth. Datapoints in this figure portion are colored only to differentiate ages from each other. (b) Plot of eyeball size versus the size of the three jaw-adductor groups, mAME (black), mAMI (red), and mAMP (blue). (c) Plot of eye size versus the individual jaw muscles we tracked, mAMEM (light gray), mAMEP (dark gray), mAMES (black), mAMP (blue), mPSTp (gold), mPSTs (red), and mPT (magenta). Note that the three components of mAME were not unequivocally separable in any of the four specimens across embryonic days 9 and 12, nor in one specimen at embryonic day 15, so regression lines for mAMEM, mAMEP, and mAMES were estimated with 13 datapoints rather than the full 18. mAME; musculus adductor mandibulae externus; mAMEM, musculus adductor mandibulae externus medialis; mAMEP, musculus adductor mandibulae externus profundus; mAMES, musculus adductor mandibulae externus superficialis; mAMI, musculus adductor mandibulae internus; mAMP, musculus adductor mandibulae posterior; mPSTp, musculus pseudotemporalis profundus; mPSTs, musculus pseudotemporalis superficialis; mPT, musculus pterygoideus dorsalis.

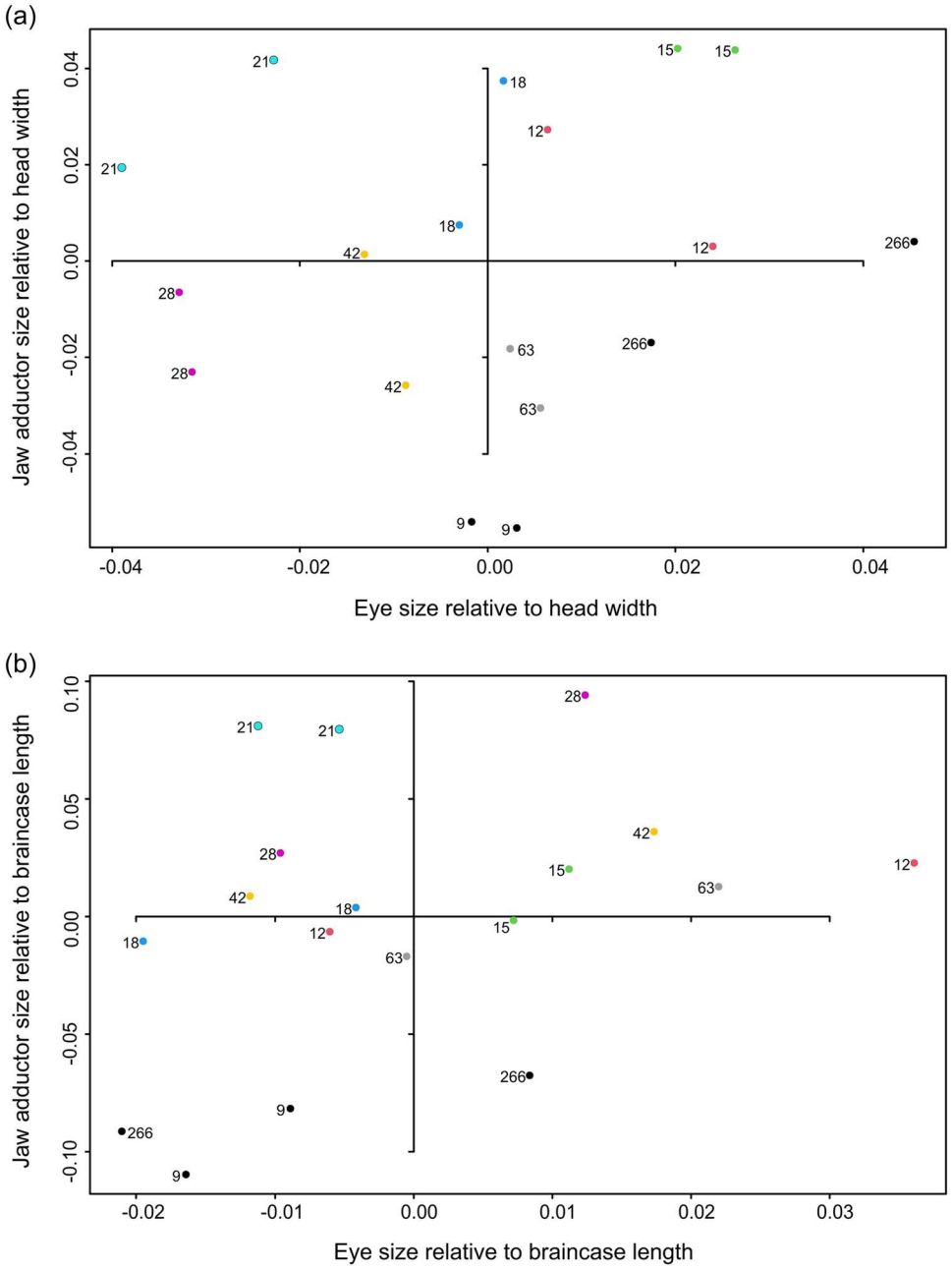

FIGURE 19 Plots of eyeball size versus jaw muscle size, with both dimensions relative to a linear dimension of the skull. (a) Plot of eye size versus jaw muscle size, with both dimensions relative to interquadrate distance. Although a relationship between these dimensions was recovered, it was a weak correlation and explained little variance. (b) Plot of eye size versus jaw muscle size, with both dimensions relative to the length of the braincase. No linear relationship between these relative dimensions was recovered. Note, however, that in both (a) and (b), eyes are consistently small (relative to the head) from just before hatching until about a week or so after hatching (days 18–28), whereas the jaw adductors are consistently large (relative to the head) on the day of hatching (day 21). In other words, growth of the jaw adductors outpaces the eye in the perinatal period.

growth sometime between the 6th- and 35th-week after hatching. The jaw muscles also grow with positive allometry relative to the width of the head and the length of the braincase, as opposed to the brain, which is negatively allometric with respect to those two dimensions of the head. Given that the *Gallus* brain fills the endocranium more in mature individuals than in developing juveniles (Watanabe et al., 2019), this result of negative allometry might seem surprising. However, the brain is negatively allometric with respect to skull length in the highly encephalized Corvidae (Schuh, 1968). Furthermore, jaw-adductor muscles of modern birds mature much later than the brain (Evans & Noden, 2006; Noden, 1983; Noden & Francis-West, 2006). Investigators also noted the reduction of the adductor chamber in birds relative to nonavian dinosaurs (Bhullar et al., 2016). Taken together, this group of muscles has a different

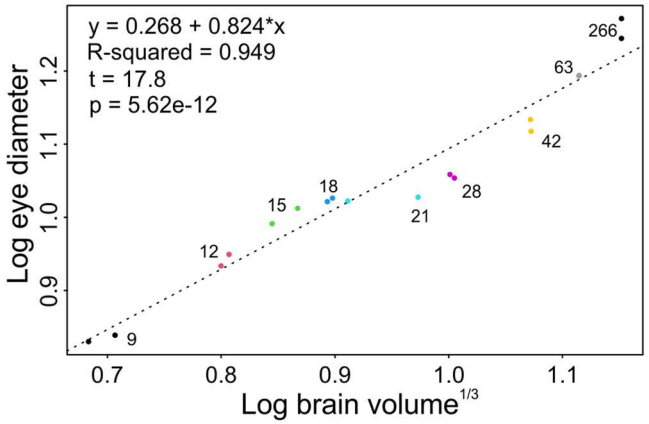

FIGURE 20 Plot of eyeball size versus brain size, showing that the eyes grow with negative allometry relative to the brain. Labels correspond to age, as follows: embryonic day 21 corresponds to the day of hatching, day 28 to 1-week after hatching, day 42 to 3-weeks after hatching, and so forth. Datapoints in this figure portion are colored only to differentiate ages from each other.

growth trajectory than the brain, directly supporting our primary alternate hypothesis (H1).

The jaw-adductor muscles also grow differently than the eyeballs. Like the brain, the eyeballs grow with overall negative allometry relative to the size of the head. The eyes, however, grow quickly before hatching, very slowly in the perinatal period, quickly again after hatching, and then level off in growth again around the third-week after hatching. Our observations on eye growth comport with past work showing that eye growth levels off as developing avian embryos approach hatching—in *Gallus* (Lindner et al., 2017; Neath et al., 1991), *Coturnix* (Arora, 2011), and *Struthio* (Brand et al., 2017). Whereas the eyes of chicks just 3 days before hatching and on the day of hatching are essentially the same size, jaw muscles from these same individuals grow consistently through the same time period. A caveat with this last observation is that the subsample of chicks at these perinatal ontogenetic stages is low ($n = 4$), so the diverging trends in eyeball and muscle growth may be due to individual variation.

We could identify most of the jaw-adductor muscles by embryonic day 9, including the mAME group, mAMP, mPSTp, mPSTs, and mPT. That we could distinguish these muscles from each other in developing embryos is concordant with Marcucio and Noden (1999), who distinguished the mAME group from the mPT and mPST groups in histological sections of embryos at embryonic day 7. Dubale and Muralidharan (1970) also distinguished these groups from each other at embryonic day 19. Discussions of earlier development of cranial muscles include, for example, Edgeworth (1907) sectioning of *Gallus* embryos from the 11-somite stage to those at embryonic day 8, and McClearn and Noden's (1988) study of the timing and patterning of myogenesis in the head muscles of quail. For a review and synthesis of these and other seminal works on the jaw-adductor musculature of birds, see Holliday and Witmer (2007).

The jaw adductors begin to closely resemble their adult shapes in chick embryos ranging from embryonic days 9–18, but the spatial orientation of the muscles shifts in more mature specimens. In particular, the ventral attachments of adductor mandibulae externus shift laterally as the skull becomes more heavily mineralized and the lower jaw becomes more robust. This change is subtle, and the overall orientation of muscle fibers remains mostly dorsoventral and rostrocaudal, as reported by Cost et al. (2022) in adult *Gallus*. However, our findings show that at least some avians experience appreciable shifts in jaw-muscle orientation during their ontogeny—shifts that visually differ from ontogenetic changes that jaw adductors go through in crocodylians, the sister group to birds (Cost et al., 2022).

4.2 | Changes to the bones of the adductor chamber

The dorsolateral aspect of the jaw-adductor chamber undergoes several ontogenetic changes, including in the size and shape of the dorsal temporal fenestra, an osteological correlate for mAME. Identity of bones that make up the fenestra and postorbital process, another osteological correlate for mAME, also shift from perinatal specimens to adults, as previously reported (Zusi, 1993). Perhaps most starkly, adult *Gallus* specimens have the most pronounced postorbital processes and medial embayments (sensu Field et al., 2018) of the upper temporal fenestra of any of the sampled specimens. Among our sample, these two features are always less pronounced in younger specimens and more obvious in older specimens. In other words, the most visible feature of the adductor chamber, the dorsal temporal fenestra, in older—but not younger—specimens more closely resembles the large adductor chambers of nonavian theropods and early ornithurans like *Ichthyornis* (Field et al., 2018).

This finding is congruent with the hypothesis that the bird head is paedomorphic by progenesis, or truncation of the plesiomorphic ontogenetic sequence (Bhullar et al., 2012, 2016; Long & McNamara, 1995; Thulborn, 1985; Weishampel & Horner, 1994). Many fossils of nonavian theropod dinosaurs and other stem avians have large jaw-adductor chambers with deep medial embayments that nearly meet midsagittally on the dorsal surface of the skull. In life, these embayments in the temporal fossa accommodated powerful jaw-closing muscles (Holliday, 2009), which would have been much larger in both relative and absolute terms than those of *Gallus*, and thus presumably grew for longer periods of time during ontogeny. If the ontogenetic sequence described for *Gallus* herein had shown rapid early growth of the jaw adductors and their osteological correlates, followed by a relative diminishment of these features later in development—a recapitulation of evolutionary changes along the avian stem—the adductor chamber could have been described as peramorphic by terminal addition (see Alberch et al., 1979). Instead, the adductor chamber in this modern bird continues growing steadily but never visibly approaches the exaggerated morphology of stem birds like nonavian theropods or

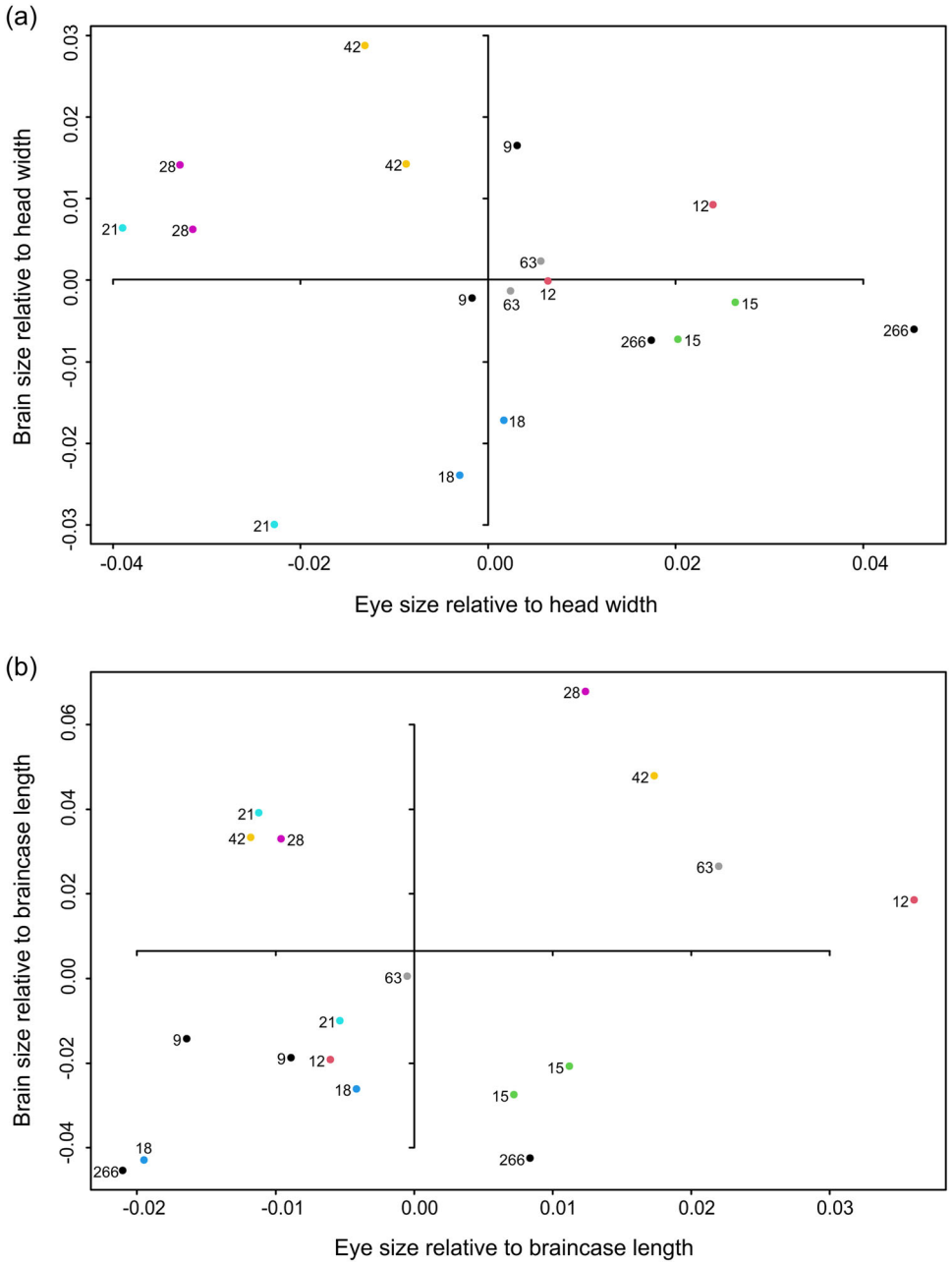

FIGURE 21 Plots of eyeball size versus brain size, with both dimensions relative to a linear dimension of the skull. (a) Plot of eye size versus brain size, with both dimensions relative to interquadrate distance. No linear relationship between these relative dimensions was recovered. (b) Plot of eye size versus brain size, with both dimensions relative to the length of the braincase. No linear relationship between these relative dimensions was recovered.

even *Ichthyornis*. This state is exactly what would be expected from a paedomorphic structure or system for which the ancestral ontogeny included a longer period of growth but has since been truncated.

4.3 | Cranial neurosensory organs and jaw adductors—Spatial packing constraints?

We collected both countervailing and supporting evidence for the idea of packing constraints on the growth of the cranial organs that we examined. There is just one inverse relationship between the size-corrected volumes of the jaw muscles and the brain, whereas all other bivariate contrasts exhibit positive or no correlation irrespective of whether measures of size are absolute or relative. In absolute terms, the jaw muscle groups grow with positive allometry at about the same rate relative to the brain and the eyes, supporting our second alternate hypothesis of nonisometry (H2) but inconsistent with the third alternate hypothesis of a difference between the muscle groups (H3). In specimens that have larger brains than expected for their braincases, the jaw adductors are

also larger than expected. This result is the opposite of what we would expect to find if the brain and jaw muscles compete for space—specifically, volume—inside the head. This absence of an inverse relationship is somewhat surprising given that there is evidence of competition for space between the brain and jaw muscles of other vertebrates. In sarcopterygians, for example, the brain more closely approximates the shape of the endocranial cavity at points where the jaw adductors attach to the cranium (Challands et al., 2020). The form of jaw adductors also impacts the shape and size of cranial sense organs like the eyes and ears, and vice versa, in cichlid fish (Barel, 1982, 1983). Even in the apparently morphologically conservative head of hammerhead sharks, the braincase imposes space constraints on other cranial organ systems (Mara et al., 2015).

More consistent with the literature on other vertebrates is our finding that the jaw adductors and brain are negatively correlated with each other when the influence of head width (interquadrate distance) is accounted for, but this finding is not without caveats. From embryonic day 15 until the third-week after hatching, when the jaw adductors are large for the head, the brain is small, and vice versa (see Figures 15 and 16a). The brain is in a phase of rapid growth during this period of time (see Figure 12a). This inverse relationship supports the idea of spatial constraints relative to the width of the head. A caveat to this discussion is that the negative correlation is poorly fit. Although the slope of the OLS regression equation is approximately −1, suggesting an even trade-off between jaw muscles and brain, the regression has a low coefficient of determination and so explains only a small proportion (~17%) of the spread in the data. The RMA slope is much steeper at about −2 but it also poorly explains spread (~20%). The poor fit of both regressions suggests that any volumetric constraints imposed by the brain and jaw muscles on each other are weak at most.

There are several plausible explanations for the observed allometric relationships between the jaw adductors, brain, and eyes. First, the jaw adductors and cranial neurosensory organs in *Gallus* are not competing for space. The brain—apart from the tracts that constitute the first two cranial nerves—is contained within the endocranial cavity, grows quickly early in development, and tapers off in its growth soon after hatching. By the time jaw-muscle primordia are detectable in diceCT-scan data, the brain is several orders of magnitude larger by volume than these early muscles. On the other hand, the jaw muscles sit external to the endocranial cavity and are bounded superficially only by skin, not bone. These two cranial physiological systems may simply be separate modules with independent growth trajectories.

Another plausible explanation—which is not incongruous with the first explanation—is that there has already been an evolutionary competition for space between these cranial systems in the *Gallus* lineage and the jaw adductors lost. Early avialans and nonavian theropod dinosaurs had relatively larger adductor chambers and relatively smaller brains than crown birds (Alonso et al., 2004; Balanoff et al., 2013; Bhullar et al., 2016; Larsson et al., 2000). These extinct groups presumably had jaw-adductor musculature that grew faster and/or for a longer period of time (i.e., different kinds of heterochrony; Dobreva et al., 2022) to reach the sizes seen in taxa like *Ichthyornis*. There is indeed evidence to suggest that the bird cranium is highly mosaic and was the subject of multiple heterochronic changes along multiple dimensions, sometimes in conflicting directions for different regions of the head (Bhullar et al., 2012, 2016; Felice & Goswami, 2017; Field et al., 2018). Early avialans may have had jaw muscles that exhibited even stronger positive allometry with respect to the size of the head than we observed in *Gallus*. Perhaps any volumetric trade-off between brain and muscles is weak in this modern taxon because these systems only minimally intrude on each other's space.

Evidence that may speak to both the first and second explanations exists. Marugán-Lobón et al. (2022) recently reported that volumetric brain growth is not the primary driver of the transformations in the avian head wrought by spatial packing constraints, which supports the explanation of no competition. Other recent work shows that the enlargement of the avian brain is less constrained by body size than in many other vertebrate groups (Tsuboi et al., 2018). Enlargement of the brain is not even quantitatively explained by a single factor like the ability to fly (Balanoff et al., 2016); instead, enlargement occurred in a mosaic pattern (Boire & Baron, 1994; Charvet & Striedter, 2009; Iwaniuk et al., 2004, 2005; Iwaniuk & Hurd, 2005). That said, the last overall shift in avian brain shape occurred near the end-Cretaceous extinction event (Torres et al., 2021), and the size of the avian brain had already increased as compared with nonavian dinosaurs by the same time (Field et al., 2018). More specifically, stem avians and early-diverging crown lineages including Galliformes passed through periods of body size decrease that outstripped brain size reduction (Ksepka et al., 2020). If a volumetric competition between the brain and jaw adductors occurred along the avian stem by the late Cretaceous and was followed by decoupling of brain and overall body sizes (our second explanation), then finding an avialan with both a large brain and large jaw muscles—whether the modern *Gallus* or an ornithuran like *Ichthyornis* (Field et al., 2018)—should be no surprise at all. These two systems were and are responding to different constraints and different selective pressures.

Of note is that *Gallus gallus* is omnivorous, eating a mix of hard seeds, plants, and both hard- and soft-bodied invertebrates (Collias & Collias, 1967; Collias & Saichuae, 1967), so we might expect this taxon to show evidence of increased investment in jaw-adductor muscles to allow for hard-shelled or -bodied food items. High bite forces were reported in certain galliform birds and some frugivorous passerines with large jaw adductors (Dzerzhinsky, 1972, 1994; Kalyakin, 2015). Furthermore, other phasianid galliforms have jaws with high mechanical advantage, which is associated with high bite force (Navalón et al., 2019). Furthermore, the jaw muscles of the ratite *Rhea americana* are reduced relative to body mass in mature individuals, which are herbivorous, compared with birds in their first few months of life, which are omnivorous and feed on harder-bodied food items (Picasso et al., 2023). If anything, these studies suggest

that the jaw muscles in *Gallus* may be more developed, not less, than their ancestors on the galliform or avian stems.

A third plausible explanation is that the brain and eyeballs may impose spatial constraints on each other but not on the jaw-adductor muscles, but the evidence for this explanation is not strong from our study. The eyeballs grow with negative allometry relative to the brain, directly supporting our fourth hypothesis of nonisometry (H4). However, there are no clear inverse relationships between the relative sizes of brain and eyes; that is, brains are not generally large for the head when eyes are small. We would expect to recover such an inverse relationship if the brain and eyes limited each other's growth across the entirety of ontogeny. Nevertheless, it is noteworthy that, relative to head width, the eyes are small at a time when the brain is large and undergoing rapid growth: at hatching and for a few weeks afterward (see Figure 21a). Given that there is evidence that the shapes of the bird orbit and brain covary (Kawabe et al., 2013), it would not be surprising if the soft-tissue eyeball is also morphometrically influenced by the brain during development. Perhaps this influence is simply temporally limited to the early postnatal time period.

A fourth plausible explanation is that spatial packing constraints on avian jaw-adductor muscles do exist but are limited, perhaps in one of the following ways: such constraints (i) may involve a different neurosensory system (the eyes), (ii) could impact shape rather than size, (iii) and/or may be limited temporally to the perinatal period. The eye, like the brain, grows quickly early in development. Even the already-well-developed extraocular muscles, which become dwarfed by mPT and mAME in adults, are much larger than the jaw-muscle primordia in the youngest embryos we studied. However, in the perinatal time period, the eyeballs increase in size little and are small relative to the head, whereas the jaw muscles are relatively large. When we consider that the jaw adductors and eyeball both take up space inside the orbit, this difference in relative size at this range of developmental stages suggests a partitioning of resources towards the jaw apparatus and away from the development of the visual system during the perinatal period. Such a partitioning could be explained by the increased use of the jaw apparatus in the days leading up to hatching. Developing chicks do use their jaw adductors during the 3 days that precede hatching, particularly for "beak clapping," or rapid open-and-shut movements of the jaws, which is presumed to thin the outer shell membrane (Hamburger & Oppenheim, 1967). Similarly, relative to head width, the jaw muscles are large and brain small just before hatching, whereas the reverse is true after hatching. This correlation, though poorly fit to the data, supports the idea of additional developmental resources being supplied to the jaw muscles perinatally.

Furthermore, if the pause in diametral growth of chick eyes discussed in 4.1 represents a programmed ontogenetic event, it would be congruent with the literature on the optical development of the eye of *G. gallus*. The *G. gallus* chick is precocial, and precocial birds at hatching have open eyes, can walk, and are at least somewhat independent of their parents with respect to acquiring food (Pough et al., 2005). Subsequent growth of the eyeball depends in part on multifactorial feedback from the retina (Flitcroft, 2012). Chicks raised experimentally with apparatus that restrict the visual field develop myopic eyes (Wallman & Adams, 1987) that are enlarged in axial length and/or diameter (Hodos & Kuenzel, 1984). Eyeball size and choroidal thickness also vary with circadian light-dark cycles (Nickla et al., 1998; Papastergiou et al., 1998). Some ground-dwelling bird species, including *G. gallus*, have eyes with lower-field myopia that is stronger at younger ages when birds are closer to the ground, which may be an adaptive phenomenon (Fitzke et al., 1985; Hodos & Erichsen, 1990). It would be no surprise at all, based on these studies, if the eyeball were developmentally programmed to pause in its growth, just before hatching, until the retina begins to receive more sensory data after hatching. The jaw adductors, meanwhile, would be free to continue growing.

The changes in muscle orientation (i.e., shape) noted in 4.1 and depicted in Figures 3, 4, and 10 may also result in part from packing constraints. There is evidence for spatial packing constraints in the bird head (Bronzati et al., 2021; Chiappe et al., 2022; Marugán-Lobón et al., 2022), but the volumetric growth of the brain alone simply does not seem to be the main driver (Marugán-Lobón et al., 2022). Given the apposition of the eyeball and jaw adductors in the orbit, perhaps these shifts represent a trade-off in force that the muscles can produce. Likewise, it would not be surprising to see shifts in jaw muscle orientation, and perhaps quantitative measure of muscle force, paralleling the diversity of avian endocranial shapes (see fig. 6 in Early et al., 2020). Although the measurement of muscle force was beyond the scope of the current study, such a study could shed light on this issue.

In summary, the results are consistent with the ideas that the jaw adductors of *G. gallus* are relatively well-developed and that there are few, if any, clear trade-offs in overall size between jaw adductors, brain, and eyes across *Gallus* ontogeny using the metrics from this study. The jaw muscles nevertheless may receive increased investment of developmental resources at the expense of investment in the eyeball at a crucial phase, perinatally. On the other hand, it was suggested that an evolutionary increase in the size of the avian eye was a driver of the kinetic nature of the bird skull and of reductions in the jaw muscles (see Bout & Zweers, 2001, for discussion and review). Similar arguments were made about lepidosaurs, wherein evidence from geckoes suggests that constructional constraints on the size of the eyeball and pennation of jaw muscles resulted in an evolutionary loss of cranial skeletal elements and an evolutionary gain of cranial kinesis in these squamates (Herrel et al., 2000).

It stands to reason that if such evolutionary trade-offs did and still do take place, we would expect to see different patterns of jaw muscle development (relative to the sensory organs), and perhaps stronger evidence of spatial constraints, in other bird species. Moreover, quantifying the use of jaw adductors by measuring bite force would shed light on the functional context in which differences in size and growth may be discovered. Measuring bite force in galliform birds in a behavioral framework would thus be a logical next step to assess the influence of functional demands (sensu Barel, 1982) on the form of the brain, eyes, and jaw adductors. Bite force has not

been behaviorally determined for *G. gallus*, although there are estimates based on anatomical measurements (Deeming et al., 2022). In truth, almost all behavioral measurements of bite force in birds were made in songbirds and birds of prey (Deeming et al., 2022). Bite-force data plus ontogenetic series of songbirds, birds of prey, and other avian species, including those birds that forage for more soft-bodied food items and those birds considered to be highly intelligent, would, with the results from the present study, bracket the last common ancestor of crown birds and allow for inferences to be made about these dynamics between the cranial neurosensory organs and jaw muscles of the earliest birds.

5 | CONCLUSIONS

This study examines the ontogenetic trajectory of the jaw-adductor muscles and the brain of *Gallus*, and it finds some evidence of a competition between the brain and jaw muscles for space within the head of this taxon. Quantitative results include a negative correlation between brain and muscles with respect to head width, but also a stronger positive correlation between these organs with respect to braincase length. Qualitative evidence is presented to suggest that at least some of the changes in the spatial disposition of the jaw muscles are related to transformations in the laterosphenoid, squamosal, and mandible over ontogeny. Implications for the anatomy of fossil avian specimens are discussed, primarily stating that the juxtaposition of derived (large) endocranium and plesiomorphic (large) space for the jaw adductors should not be surprising given the hypothesis that many elements in the bird cranium are paedomorphic.

AUTHOR CONTRIBUTIONS

Donald G. Cerio: Conceptualization; writing—review and editing; writing—original draft; visualization; investigation; formal analysis; methodology. **Catherine J. Llera Martín**: Conceptualization; writing—review and editing; writing—original draft; visualization; investigation; formal analysis; methodology. **Aneila V. C. Hogan**: Writing—review and editing; Investigation. **Amy M. Balanoff**: Conceptualization; writing—review and editing; methodology; funding acquisition. **Akinobu Watanabe**: Writing—review and editing; resources; funding acquisition. **Gabriel S. Bever**: Conceptualization; writing—original draft; writing—review and editing; funding acquisition; software; resources; methodology.

ACKNOWLEDGMENTS

This study was supported through funding from NSF DEB-1947025 (to Gabriel S. Bever), NSF DEB-1457181 (to Amy M. Balanoff, Akinobu Watanabe, and Gabriel S. Bever), NSF DEB-1406849 (to Akinobu Watanabe), the Mary R. Dawson Predoctoral Fellowship Grant through the Society of Vertebrate Paleontology (to Akinobu Watanabe), and the Comparative Biology Program at the Richard Gilder Graduate School (to Akinobu Watanabe). The authors thank Paul Gignac for assistance with diceCT, as well as Vera Weisbecker and Alison Carlisle for assistance with the STABILITY hydrogel protocol. The authors also thank E. J. Huang, Jacob Wilson, Fernando Torres, and William Foster for their helpful comments and discussion, which improved the manuscript. The authors also thank the reviewers for their helpful comments, which improved the manuscript.

CONFLICT OF INTEREST STATEMENT

The authors declare no conflict of interest.

DATA AVAILABILITY STATEMENT

A spreadsheet of raw linear and volumetric measurements, the R code for statistical analyses, and surface meshes of the segmented jaw-adductor muscles are available as supporting material associated with this article.

ORCID

Donald G. Cerio http://orcid.org/0000-0002-7517-5791

Catherine J. Llera Martín http://orcid.org/0000-0002-5822-3595

REFERENCES

Alberch, P., Gould, S. J., Oster, G. F., & Wake, D. B. (1979). Size and shape in ontogeny and phylogeny. *Paleobiology*, *5*(3), 296–317. https://doi.org/10.1017/S0094837300006588

Alexander, R. M., Jayes, A. S., Maloiy, G. M. O., & Wathuta, E. M. (1981). Allometry of the leg muscles of mammals. *Journal of Zoology*, *194*(4), 539–552. https://doi.org/10.1111/j.1469-7998.1981.tb04600.x

Alonso, P. D., Milner, A. C., Ketcham, R. A., Cookson, M. J., & Rowe, T. B. (2004). The avian nature of the brain and inner ear of *Archaeopteryx*. *Nature*, *430*(7000), 666–669. https://doi.org/10.1038/nature02706

Arora, K. L. (2011). Allometric growth of prenatal organs as a function of age in the Japanese quail embryo, *Coturnix japonica*. *International Journal of Poultry Science*, *10*, 300–308.

Balanoff, A. M., & Bever, G. S. (2017). The role of endocasts in the study of brain evolution. In J. H. Kaas (Ed.), *Evolution of nervous systems* (pp. 223–241). Elsevier. https://doi.org/10.1016/B978-0-12-804042-3.00023-3

Balanoff, A. M., Bever, G. S., Rowe, T. B., & Norell, M. A. (2013). Evolutionary origins of the avian brain. *Nature*, *501*(7465), 93–96. https://doi.org/10.1038/nature12424

Balanoff, A. M., Smaers, J. B., & Turner, A. H. (2016). Brain modularity across the theropod–bird transition: Testing the influence of flight on neuroanatomical variation. *Journal of Anatomy*, *229*(2), 204–214. https://doi.org/10.1111/joa.12403

Barel, C. D. N. (1982). Towards a constructional morphology of cichlid fishes (Teleostei, Perciformes). *Netherlands Journal of Zoology*, *33*(4), 357–424. https://doi.org/10.1163/002829683X00183

Barel, C. D. N. (1983). Form-relations in the context of constructional morphology: The eye and suspensorium of lacustrine Cichlidae (Pisces, Teleostei). *Netherlands Journal of Zoology*, *34*(4), 439–502. https://doi.org/10.1163/002829684X00263

Baumel, J. J., & Witmer, L. M. (1993). Osteologia. In J. J. Baumel, A. S. King, J. E. Breazile, H. E. Evans, & J. C. Vanden Berge (Eds.), *Nomina Anatomica Avium* (2nd ed., pp. 45–132). Nuttall Ornithological Club.

Bennett, M. B. (1996). Allometry of the leg muscles of birds. *Journal of Zoology*, *238*(3), 435–443. https://doi.org/10.1111/j.1469-7998.1996.tb05404.x

Bennett, P. M., & Harvey, P. H. (1985). Brain size, development and metabolism in birds and mammals. *Journal of Zoology*, *207*(4), 491–509. https://doi.org/10.1111/j.1469-7998.1985.tb04946.x

Benson, R. B. J., Campione, N. E., Carrano, M. T., Mannion, P. D., Sullivan, C., Upchurch, P., & Evans, D. C. (2014). Rates of dinosaur body mass evolution indicate 170 million years of sustained

ecological innovation on the avian stem lineage. *PLoS Biology*, *12*(5), e1001853. https://doi.org/10.1371/journal.pbio.1001853

Bhullar, B.-A. S., Hanson, M., Fabbri, M., Pritchard, A., Bever, G. S., & Hoffman, E. (2016). How to make a bird skull: Major transitions in the evolution of the avian cranium, paedomorphosis, and the beak as a surrogate hand. *Integrative and Comparative Biology*, *56*(3), 389–403. https://doi.org/10.1093/icb/icw069

Bhullar, B.-A. S., Marugán-Lobón, J., Racimo, F., Bever, G. S., Rowe, T. B., Norell, M. A., & Abzhanov, A. (2012). Birds have paedomorphic dinosaur skulls. *Nature*, *487*(7406), 223–226. https://doi.org/10.1038/nature11146

Biegert, J. (1957). Der Formwandel der Primatenschädels und seine Beziehungen zur ontogenetischen (Entwicklung und den phylogenetischen Spezialisationes der Kopforgane). *Gegenbaurs Morphologisches Jahrbuch*, *98*, 77–199.

Boire, D., & Baron, G. (1994). Allometric comparison of brain and main brain subdivisions in birds. *Journal fur Hirnforschung*, *35*(1), 49–66.

Bout, R. G., & Zweers, G. A. (2001). The role of cranial kinesis in birds. *Comparative Biochemistry and Physiology. Part A, Molecular & Integrative Physiology*, *131*(1), 197–205. https://doi.org/10.1016/S1095-6433(01)00470-6

Brand, Z., Cloete, S. W. P., Malecki, I. A., & Brown, C. R. (2017). Ostrich (*Struthio camelus*) embryonic development from 7 to 42 days of incubation. *British Poultry Science*, *58*, 139–143.

Bronzati, M., Benson, R. B. J., Evers, S. W., Ezcurra, M. D., Cabreira, S. F., Choiniere, J., Dollman, K. N., Paulina-Carabajal, A., Radermacher, V. J., Roberto-da-Silva, L., Sobral, G., Stocker, M. R., Witmer, L. M., Langer, M. C., & Nesbitt, S. J. (2021). Deep evolutionary diversification of semicircular canals in archosaurs. *Current Biology*, *31*(12), 2520–2529. https://doi.org/10.1016/j.cub.2021.03.086

Brooke, M. de L., Hanley, S., & Laughlin, S. B. (1999). The scaling of eye size with body mass in birds. *Proceedings of the Royal Society B: Biological Sciences*, *266*(1417), 405–412. https://doi.org/10.1098/rspb.1999.0652

Burt, D. W. (2007). Emergence of the chicken as a model organism: Implications for agriculture and biology. *Poultry Science*, *86*(7), 1460–1471. https://doi.org/10.1093/ps/86.7.1460

Burton, R. F. (2008). The scaling of eye size in adult birds: Relationship to brain, head and body sizes. *Vision Research*, *48*(22), 2345–2351. https://doi.org/10.1016/j.visres.2008.08.001

Carlisle, A., Selwood, L., Hinds, L. A., Saunders, N., Habgood, M., Mardon, K., & Weisbecker, V. (2017). Testing hypotheses of developmental constraints on mammalian brain partition evolution, using marsupials. *Scientific Reports*, *7*(1), 4241. https://doi.org/10.1038/s41598-017-02726-9

Carlisle, A., & Weisbecker, V. (2016). *A modified STABILITY protocol for accurate retrieval of soft-tissue data from micro-CT scans of IKI-stained specimens*. https://dicect.com/2016/08/09/stability/

Challands, T. J., Pardo, J. D., & Clement, A. M. (2020). Mandibular musculature constrains brain–endocast disparity between sarcopterygians. *Royal Society Open Science*, *7*(9), 200933. https://doi.org/10.1098/rsos.200933

Charvet, C. J., & Striedter, G. F. (2009). Developmental basis for telencephalon expansion in waterfowl: Enlargement prior to neurogenesis. *Proceedings of the Royal Society B: Biological Sciences*, *276*(1672), 3421–3427. https://doi.org/10.1098/rspb.2009.0888

Chiappe, L. M., Navalón, G., Martinelli, A. G., Nava, W., & Field, D. J. (2022). Fossil basicranium clarifies the origin of the avian central nervous system and inner ear. *Proceedings of the Royal Society B: Biological Sciences*, *289*(1983), 20221398. https://doi.org/10.1098/rspb.2022.1398

Collias, N. E., & Collias, E. C. (1967). A field study of the red jungle fowl in north-central India. *The Condor*, *69*(4), 360–386. https://doi.org/10.2307/1366199

Collias, N. E., & Saichuae, P. (1967). Ecology of the red jungle fowl in Thailand and Malaya with reference to the origin of domestication. *Natural History Bulletin of the Siam Society*, *22*, 189–209.

Cost, I. N., Sellers, K. C., Rozin, R. E., Spates, A. T., Middleton, K. M., & Holliday, C. M. (2022). 2D and 3D visualizations of archosaur jaw muscle mechanics, ontogeny and phylogeny using ternary diagrams and 3D modeling. *Journal of Experimental Biology*, *225*, jeb243216. https://doi.org/10.1242/jeb.243216

Deeming, D. C., Harrison, S. L., & Sutton, G. P. (2022). Inter-relationships among body mass, jaw musculature and bite force in birds. *Journal of Zoology*, *317*, 129–137. https://doi.org/10.1111/jzo.12966

Dobreva, M. P., Camacho, J., & Abzhanov, A. (2022). Time to synchronize our clocks: Connecting developmental mechanisms and evolutionary consequences of heterochrony. *Journal of Experimental Zoology Part B: Molecular and Developmental Evolution*, *338*(1–2), 87–106. https://doi.org/10.1002/jez.b.23103

Dubale, M. S., & Muralidharan, P. (1970). Histochemical studies on the fiber types in the developing jaw-muscles of domestic fowl (*Gallus domesticus*). *Life Sciences*, *9*(16), 949–959. https://doi.org/10.1016/0024-3205(70)90066-4

Dzerzhinsky, F. Y. (1972). *Biomechanical analysis of bird jaw apparatus*. Publishing House of Moscow State University.

Dzerzhinsky, F. Y. A. (1994). Trophic specialization characteristics of crested argus (*Rheinartia ocellata*) from South Vietnam in the light of the jaws apparatus morphology. In A. N. Tikhonov & V. A. Sadovnichy (Eds.), *Biology, ecology, biotechnology and pedology* (pp. 92–105). Russian Universities Program, Publishing House of Moscow State University.

Early, C. M., Ridgely, R. C., & Witmer, L. M. (2020). Beyond endocasts: Using predicted brain-structure volumes of extinct birds to assess neuroanatomical and behavioral inferences. *Diversity*, *12*(1), 34. https://doi.org/10.3390/d12010034

Edgeworth, F. H. (1907). Memoirs: The development of the head-muscles in *Gallus domesticus*, and the morphology of the head-muscles in the Sauropsida. *Journal of Cell Science*, *s2-51*(204), 511–556. https://doi.org/10.1242/jcs.s2-51.204.511

Elzanowski, A. (1993). Interconnections of muscles in the adductor mandibulae complex of birds. *Annals of Anatomy—Anatomischer Anzeiger*, *175*(1), 29–34. https://doi.org/10.1016/S0940-9602(11)80233-5

Evans, D. J. R., & Noden, D. M. (2006). Spatial relations between avian craniofacial neural crest and paraxial mesoderm cells. *Developmental Dynamics*, *235*(5), 1310–1325. https://doi.org/10.1002/dvdy.20663

Fabbri, M., Mongiardino Koch, N., Pritchard, A. C., Hanson, M., Hoffman, E., Bever, G. S., Balanoff, A. M., Morris, Z. S., Field, D. J., Camacho, J., Rowe, T. B., Norell, M. A., Smith, R. M., Abzhanov, A., & Bhullar, B. S. (2017). The skull roof tracks the brain during the evolution and development of reptiles including birds. *Nature Ecology & Evolution*, *1*(10), 1543–1550. https://doi.org/10.1038/s41559-017-0288-2

Felice, R. N., & Goswami, A. (2017). Developmental origins of mosaic evolution in the avian cranium. *Proceedings of the National Academy of Sciences*, *115*(3), 555–560. https://doi.org/10.1073/pnas.1716437115

Field, D. J., Hanson, M., Burnham, D., Wilson, L. E., Super, K., Ehret, D., Ebersole, J. A., & Bhullar, B. A. S. (2018). Complete *Ichthyornis* skull illuminates mosaic assembly of the avian head. *Nature*, *557*(7703), 96–100. https://doi.org/10.1038/s41586-018-0053-y

Fitzke, F. W., Hayes, B. P., Hodos, W., Holden, A. L., & Low, J. C. (1985). Refractive sectors in the visual field of the pigeon eye. *The Journal of Physiology*, *369*(1), 33–44. https://doi.org/10.1113/jphysiol.1985.sp015886

Flitcroft, D. I. (2012). The complex interactions of retinal, optical and environmental factors in myopia aetiology. *Progress in Retinal and Eye Research*, *31*(6), 622–660. https://doi.org/10.1016/j.preteyeres.2012.06.004

Fox, J., & Weisberg, S. (2019). *An R companion to applied regression* (3rd ed.). SAGE.

Gignac, P. M., Kley, N. J., Clarke, J. A., Colbert, M. W., Morhardt, A. C., Cerio, D., Cost, I. N., Cox, P. G., Daza, J. D., Early, C. M., Echols, M. S., Henkelman, R. M., Herdina, A. N., Holliday, C. M., Li, Z., Mahlow, K., Merchant, S., Müller, J., Orsbon, C. P., … Witmer, L. M. (2016). Diffusible iodine-based contrast-enhanced computed tomography (diceCT): An emerging tool for rapid, high-resolution, 3-D imaging of metazoan soft tissues. *Journal of Anatomy*, *228*(6), 889–909. https://doi.org/10.1111/joa.12449

Gould, S. J. (1977). *Ontogeny and phylogeny*. The Belknap Press of Harvard University Press.

Hamburger, V., & Oppenheim, R. (1967). Prehatching motility and hatching behavior in the chick. *Journal of Experimental Zoology*, *166*(2), 171–203. https://doi.org/10.1002/jez.1401660203

Herrel, A., Aerts, P., & De Vree, F. (2000). Cranial kinesis in geckoes: Functional implications. *Journal of Experimental Biology*, *203*(9), 1415–1423. https://doi.org/10.1242/jeb.203.9.1415

Hodos, W., & Erichsen, J. T. (1990). Lower-field myopia in birds: An adaptation that keeps the ground in focus. *Vision Research*, *30*(5), 653–657. https://doi.org/10.1016/0042-6989(90)90091-X

Hodos, W., & Kuenzel, W. J. (1984). Retinal-image degradation produces ocular enlargement in chicks. *Investigative Ophthalmology & Visual Science*, *25*(6), 652–659. https://iovs.arvojournals.org/article.aspx?articleid=2159489

Hogan, A. V. C., Watanabe, A., Balanoff, A. M., & Bever, G. S. (2020). Comparative growth in the olfactory system of the developing chick with considerations for evolutionary studies. *Journal of Anatomy*, *237*(2), 225–240. https://doi.org/10.1111/joa.13197

Holliday, C. M. (2009). New insights into dinosaur jaw muscle anatomy. *The Anatomical Record: Advances in Integrative Anatomy and Evolutionary Biology*, *292*(9), 1246–1265. https://doi.org/10.1002/ar.20982

Holliday, C. M., & Witmer, L. M. (2007). Archosaur adductor chamber evolution: Integration of musculoskeletal and topological criteria in jaw muscle homology. *Journal of Morphology*, *268*(6), 457–484. https://doi.org/10.1002/jmor.10524

Iwaniuk, A. N. (2017). Functional correlates of brain and brain region sizes in nonmammalian vertebrates. In *Evolution of nervous systems* (pp. 335–348). Elsevier. https://doi.org/10.1016/B978-0-12-804042-3.00024-5

Iwaniuk, A. N., Dean, K. M., & Nelson, J. E. (2004). A mosaic pattern characterizes the evolution of the avian brain. *Proceedings of the Royal Society of London. Series B: Biological Sciences*, *271*(suppl_4), S148–S151. https://doi.org/10.1098/rsbl.2003.0127

Iwaniuk, A. N., Dean, K. M., & Nelson, J. E. (2005). Interspecific allometry of the brain and brain regions in parrots (Psittaciformes): Comparisons with other birds and primates. *Brain, Behavior and Evolution*, *65*(1), 40–59. https://doi.org/10.1159/000081110

Iwaniuk, A. N., & Hurd, P. L. (2005). The evolution of cerebrotypes in birds. *Brain, Behavior and Evolution*, *65*(4), 215–230. https://doi.org/10.1159/000084313

Kalyakin, M. V. (2015). Morpho-functional analysis of the jaw apparatus of Vietnamese Passerine birds (Passeriformes): Inferences on their trophic adaptations, ecology, and systematic position. *Journal of Ornithology*, *156*(S1), 307–315. https://doi.org/10.1007/s10336-015-1246-x

Kawabe, S., Shimokawa, T., Miki, H., Matsuda, S., & Endo, H. (2013). Variation in avian brain shape: Relationship with size and orbital shape. *Journal of Anatomy*, *223*, 495–508. https://doi.org/10.1111/joa.12109

Kiecker, C. (2016). The chick embryo as a model for the effects of prenatal exposure to alcohol on craniofacial development. *Developmental Biology*, *415*(2), 314–325. https://doi.org/10.1016/j.ydbio.2016.01.007

Kiltie, R. A. (2000). Scaling of visual acuity with body size in mammals and birds. *Functional Ecology*, *14*(2), 226–234. https://doi.org/10.1046/j.1365-2435.2000.00404.x

Ksepka, D. T., Balanoff, A. M., Smith, N. A., Bever, G. S., Bhullar, B.-A. S., Bourdon, E., Braun, E. L., Burleigh, J. G., Clarke, J. A., Colbert, M. W., Corfield, J. R., Degrange, F. J., De Pietri, V. L., Early, C. M., Field, D. J., Gignac, P. M., Gold, M. E. L., Kimball, R. T., Kawabe, S., … Smaers, J. B. (2020). Tempo and pattern of avian brain size evolution. *Current Biology*, *30*(11), 2026–2036. https://doi.org/10.1016/j.cub.2020.03.060

Larsson, H. C. E., Sereno, P. C., & Wilson, J. A. (2000). Forebrain enlargement among nonavian theropod dinosaurs. *Journal of Vertebrate Paleontology*, *20*(3), 615–618. https://doi.org/10.1671/0272-4634(2000)020[0615:FEANTD]2.0.CO;2

Lee, M. S. Y., Cau, A., Naish, D., & Dyke, G. J. (2014). Sustained miniaturization and anatomical innovation in the dinosaurian ancestors of birds. *Science*, *345*(6196), 562–566. https://doi.org/10.1126/science.1252243

Legendre, P. (2018). *lmodel2: Model II Regression* [R]. https://CRAN.R-project.org/package=lmodel2

Lessner, E. J., & Holliday, C. M. (2020). A 3D ontogenetic atlas of *Alligator mississippiensis* cranial nerves and their significance for comparative neurology of reptiles. *The Anatomical Record*, *305*, 2854–2882. https://doi.org/10.1002/ar.24550

Liem, K. F., & Wake, D. B. (1985). Morphology: Current approaches and concepts. In D. M. Bramble, M. Hildebrand, K. F. Liem, & D. B. Wake (Eds.), *Functional vertebrate morphology* (pp. 366–414). Harvard University Press. https://doi.org/10.4159/harvard.9780674184404

Lindner, T., Klose, R., Streckenbach, F., Stahnke, T., Hadlich, S., Kühn, J.-P., Guthoff, R. F., Wree, A., Neumann, A. M., Frank, M., Glass, Ä., Langner, S., & Stachs, O. (2017). Morphologic and biometric evaluation of chick embryo eyes in ovo using 7 Tesla MRI. *Scientific Reports*, *7*, 2647.

Long, J., & McNamara, K. (1995). Heterochrony in dinosaur evolution. In K. McNamara (Ed.), *Evolutionary change and heterochrony* (pp. 151–168). Wiley.

Maloiy, G. M. O., Alexander, R. M., Njau, R., & Jayes, A. S. (1979). Allometry of the legs of running birds. *Journal of Zoology*, *187*(2), 161–167. https://doi.org/10.1111/j.1469-7998.1979.tb03940.x

Mara, K. R., Motta, P. J., Martin, A. P., & Hueter, R. E. (2015). Constructional morphology within the head of hammerhead sharks (Sphyrnidae): Cranial morphology in hammerhead sharks. *Journal of Morphology*, *276*(5), 526–539. https://doi.org/10.1002/jmor.20362

Marcucio, R. S., & Noden, D. M. (1999). Myotube heterogeneity in developing chick craniofacial skeletal muscles. *Developmental Dynamics*, *214*(3), 178–194. https://doi.org/10.1002/(SICI)1097-0177(199903)214:3<178::AID-AJA2>3.0.CO;2-4

Martin, G. R. (1985). Eye. In A. S. King & J. McLelland (Eds.), *Form and function in birds* (pp. 311–373). Academic Press.

Marugán-Lobón, J., Nebreda, S. M., Navalón, G., & Benson, R. B. J. (2022). Beyond the beak: Brain size and allometry in avian craniofacial evolution. *Journal of Anatomy*, *240*(2), 197–209. https://doi.org/10.1111/joa.13555

McClearn, D., & Noden, D. M. (1988). Ontogeny of architectural complexity in embryonic quail visceral arch muscles. *American Journal of Anatomy*, *183*(4), 277–293. https://doi.org/10.1002/aja.1001830402

van der Meij, M. A. A., & Bout, R. G. (2004). Scaling of jaw muscle size and maximal bite force in finches. *Journal of Experimental Biology*, *207*(16), 2745–2753. https://doi.org/10.1242/jeb.01091

Navalón, G., Bright, J. A., Marugán-Lobón, J., & Rayfield, E. J. (2019). The evolutionary relationship among beak shape, mechanical advantage, and feeding ecology in modern birds. *Evolution*, *73*(3), 422–435. https://doi.org/10.1111/evo.13655

Neath, P., Roche, S. M., & Bee, J. A. (1991). Intraocular pressure-dependent and -independent phases of growth of the embryonic chick eye and cornea. *Investigative Ophthalmology & Visual Science*, *32*, 2483–2491.

Nickla, D. L., Wildsoet, C., & Wallman, J. (1998). Visual influences on diurnal rhythms in ocular length and choroidal thickness in chick eyes. *Experimental Eye Research*, *66*(2), 163–181. https://doi.org/10.1006/exer.1997.0420

Noden, D. M. (1983). The embryonic origins of avian cephalic and cervical muscles and associated connective tissues. *American Journal of Anatomy*, *168*(3), 257–276. https://doi.org/10.1002/aja.1001680302

Noden, D. M., & Francis-West, P. (2006). The differentiation and morphogenesis of craniofacial muscles. *Developmental Dynamics*, *235*(5), 1194–1218. https://doi.org/10.1002/dvdy.20697

O'Brien, H. D., Lynch, L. M., Vliet, K. A., Brueggen, J., Erickson, G. M., & Gignac, P. M. (2019). Crocodylian head width allometry and phylogenetic prediction of body size in extinct crocodyliforms. *Integrative Organismal Biology*, *1*(1), obz006. https://doi.org/10.1093/iob/obz006

Papastergiou, G. I., Schmid, G. F., Riva, C. E., Mendel, M. J., Stone, R. A., & Laties, A. M. (1998). Ocular axial length and choroidal thickness in newly hatched chicks and one-year-old chickens fluctuate in a diurnal pattern that is influenced by visual experience and intraocular pressure changes. *Experimental Eye Research*, *66*(2), 195–205. https://doi.org/10.1006/exer.1997.0421

Picasso, M. B. J., Mosto, C., & Tudisca, A. M. (2023). The feeding apparatus of *Rhea americana* (Aves, Palaeognathae): Jaw myology and ontogenetic allometry. *Journal of Morphology*, *284*(7), e21596. https://doi.org/10.1002/jmor.21596

Pough, F. H., Janis, C. M., & Heiser, J. B. (2005). *Vertebrate life* (7th ed.). Pearson/Prentice Hall.

R Core Team. (2022). *R: A language and environment for statistical computing*. R Foundation for Statistical Computing. https://www.R-project.org/

Ross, C. F., & Ravosa, M. J. (1993). Basicranial flexion, relative brain size, and facial kyphosis in nonhuman primates. *American Journal of Physical Anthropology*, *91*(3), 305–324. https://doi.org/10.1002/ajpa.1330910306

Schuh, J. (1968). Allometrische Untersuchungen über den Formenwandel des Schädels von Corviden. *Zeitschrift Für Wissenschaftliche Zoologie, Abteilung A*, *177*(1–2), 97–182.

Seilacher, A. (1970). Arbeitskonzept zur Konstruktions-Morphologie. *Lethaia*, *3*(4), 393–396. https://doi.org/10.1111/j.1502-3931.1970.tb00830.x

Shatkovska, O. V., & Ghazali, M. (2020). Integration of skeletal traits in some passerines: Impact (or the lack thereof) of body mass, phylogeny, diet and habitat. *Journal of Anatomy*, *236*(2), 274–287. https://doi.org/10.1111/joa.13095

Stern, C. D. (2005). The chick: A great model system becomes even greater. *Developmental Cell*, *8*(1), 9–17. https://doi.org/10.1016/j.devcel.2004.11.018

Thulborn, T. (1985). Birds as neotenous dinosaurs. *Records of the New Zealand Geological Survey*, *9*, 90–92.

Tokita, M. (2004). Morphogenesis of parrot jaw muscles: Understanding the development of an evolutionary novelty. *Journal of Morphology*, *259*(1), 69–81. https://doi.org/10.1002/jmor.10172

Torres, C. R., Norell, M. A., & Clarke, J. A. (2021). Bird neurocranial and body mass evolution across the end-Cretaceous mass extinction: The avian brain shape left other dinosaurs behind. *Science Advances*, *7*(31), eabg7099. https://doi.org/10.1126/sciadv.abg7099

Tsuboi, M., van der Bijl, W., Kopperud, B. T., Erritzøe, J., Voje, K. L., Kotrschal, A., Yopak, K. E., Collin, S. P., Iwaniuk, A. N., & Kolm, N. (2018). Breakdown of brain–body allometry and the encephalization of birds and mammals. *Nature Ecology & Evolution*, *2*(9), 1492–1500. https://doi.org/10.1038/s41559-018-0632-1

Vogel, K. (1991). Concepts of constructional morphology. In N. Schmidt-Kittler & K. Vogel (Eds.), *Constructional morphology and evolution* (pp. 55–68). Springer. https://doi.org/10.1007/978-3-642-76156-0_5

Wallman, J., & Adams, J. I. (1987). Developmental aspects of experimental myopia in chicks: Susceptibility, recovery and relation to emmetropization. *Vision Research*, *27*(7), 1139–1163. https://doi.org/10.1016/0042-6989(87)90027-7

Walls, G. L. (1942). *The vertebrate eye and its adaptive radiation*. The Cranbrook Institute of Science.

Warton, D. I., Duursma, R. A., Falster, D. S., & Taskinen, S. (2012). smatr 3—An R package for estimation and inference about allometric lines. *Methods in Ecology and Evolution*, *3*(2), 257–259. https://doi.org/10.1111/j.2041-210X.2011.00153.x

Watanabe, A., Balanoff, A. M., Gignac, P. M., Gold, M. E. L., & Norell, M. A. (2021). Novel neuroanatomical integration and scaling define avian brain shape evolution and development. *eLife*, *10*, e68809. https://doi.org/10.7554/eLife.68809

Watanabe, A., Gignac, P. M., Balanoff, A. M., Green, T. L., Kley, N. J., & Norell, M. A. (2019). Are endocasts good proxies for brain size and shape in archosaurs throughout ontogeny. *Journal of Anatomy*, *234*(3), 291–305. https://doi.org/10.1111/joa.12918

Weishampel, D. B., & Horner, J. R. (1994). Life history syndromes, heterochrony, and the evolution of Dinosauria. In K. Carpenter, K. Hirsch & J. Horner (Eds.), *Dinosaur eggs and babies* (pp. 229–243). Cambridge University Press.

Witmer, L. M. (1995). The extant phylogenetic bracket and the importance of reconstructing soft tissues in fossils. *Functional Morphology in Vertebrate Paleontology*, *1*, 19–33.

Wong, M. D., Spring, S., & Henkelman, R. M. (2013). Structural stabilization of tissue for embryo phenotyping using micro-CT with iodine staining. *PLoS ONE*, *8*(12), e84321. https://doi.org/10.1371/journal.pone.0084321

Zusi, R. L. (1993). Patterns of diversity in the avian skull. In J. Hanken & B. K. Hall (Eds.), *The skull* (Vol. 2, pp. 391–437). University of Chicago Press.

SUPPORTING INFORMATION

Additional supporting information can be found online in the Supporting Information section at the end of this article.

How to cite this article: Cerio, D. G., Llera Martín, C. J., Hogan, A. V. C., Balanoff, A. M., Watanabe, A., & Bever, G. S. (2023). Differential growth of the adductor muscles, eyeball, and brain in the chick *Gallus gallus* with comments on the fossil record of stem-group birds. *Journal of Morphology*, *284*, e21622. https://doi.org/10.1002/jmor.21622